Thermo
Electron
CORPORATION

## DISCLAIMER

Thermo Electron CORPORATION

Report No. TE4258/4247-72-81

DOE/ET/11292--T4

DE81 024429



# DOE/JPL ADVANCED THERMIONIC TECHNOLOGY PROGRAM

## PROGRESS REPORT NO. 44

July, August, September
1980

DOE Contract DE-AC02-76ET11291
JPL Contract 955009

Prepared by

Thermo Electron Corporation
101 First Avenue
Waltham, Massachusetts 02254

page blank

## TABLE OF CONTENTS


| Chapter | | Page |
|---|---|---|
| | INTRODUCTION AND SUMMARY | vii |
| 1.0 | PART ONE: DOE TASKS | 1 |
| | 1.1 THERMIONIC AND MATERIAL RESEARCH AND TECHNOLOGY | 1 |
| | 1.1.1 TASK I. SURFACE AND PLASMA INVESTIGATIONS | 1 |
| | 1.1.2 TASK II. LOW-TEMPERATURE CONVERTER DEVELOPMENT | 12 |
| | A. Converter No. 246: Heat Flux Diode | 12 |
| | 1.1.3 TASK III. ENHANCED MODE CONVERTER EXPERIMENTS | 16 |
| | 1.1.4 TASK IV. COMPONENT HARDWARE DEVELOPMENT | 17 |
| | A. Alloy Hot Shell Development | 17 |
| | B. CVD Hot Shell-Emitter Development | 17 |
| | 1.2 THERMIONIC POWER MODULE EVALUATION | 28 |
| | 1.2.1 TASK V. SYSTEM STUDIES | 28 |
| | 1.2.2 TASK VI. TAM MODULE DEVELOPMENT | 29 |
| | A. Converter No. 239: One-Inch Diameter Hemispherical Silicon Carbide Converter (CVD Tungsten as Deposited Emitter, Nickel Collector) | 29 |
| | B. Converter No. 247: Two-Inch Diameter Hemispherical Silicon Carbide Converter (CVD Tungsten as Deposited Emitter, Nickel Collector) | 30 |
| | C. Design of Two-Inch Diameter Torrispherical Silicon Carbide Converter | 33 |
| | D. CVD Silicon Carbide Array Module | 33 |
| | 1.2.3 TASK VII. COAL-FIRED TAM TEST UNIT | 35 |
| 2.0 | PART TWO: NASA-OAST/JPL TASKS | 37 |
| | 2.1 THERMIONIC CONVERTER EVALUATION | 37 |

## TABLE OF CONTENTS (Continued)


| Chapter | | Page |
|---|---|---|
| | 2.1.1 TASK VIII. HIGH-TEMPERATURE CONVERTER EVALUATION | 37 |
| | A. Converter No. 242 (JPL No. 9): Tungsten Emitter, Molybdenum Oxide Collector | 37 |
| | B. Converter No. 240 (JPL No. 10): Tungsten Emitter, Molybdenum Oxide Collector | 41 |
| | C. Converter No. 241 (JPL No. 11): Tungsten Emitter, Molybdenum Oxide Collector | 50 |
| | D. Converter No. 243 (JPL No. 12): Rhenium Emitter, Molybdenum Oxide Collector | 55 |
| | 2.1.2 TASK IX. ADVANCED CONVERTER STUDIES | 61 |
| | 2.1.3 TASK X. POSTOPERATION DIAGNOSTICS | 62 |
| | 2.2 CYLINDRICAL CONVERTER DEVELOPMENT | 67 |
| | 2.2.1 TASK XI. CYLINDRICAL CONVERTER COMPONENT DEVELOPMENT | 67 |
| | 2.2.2 TASK XII. CORRELATION OF DESIGN INTERFACES | 67 |
| | REFERENCES | 73 |

# DOE Contract No. EY-76-C-02-3056
# WORK BREAKDOWN STRUCTURE

7911-11

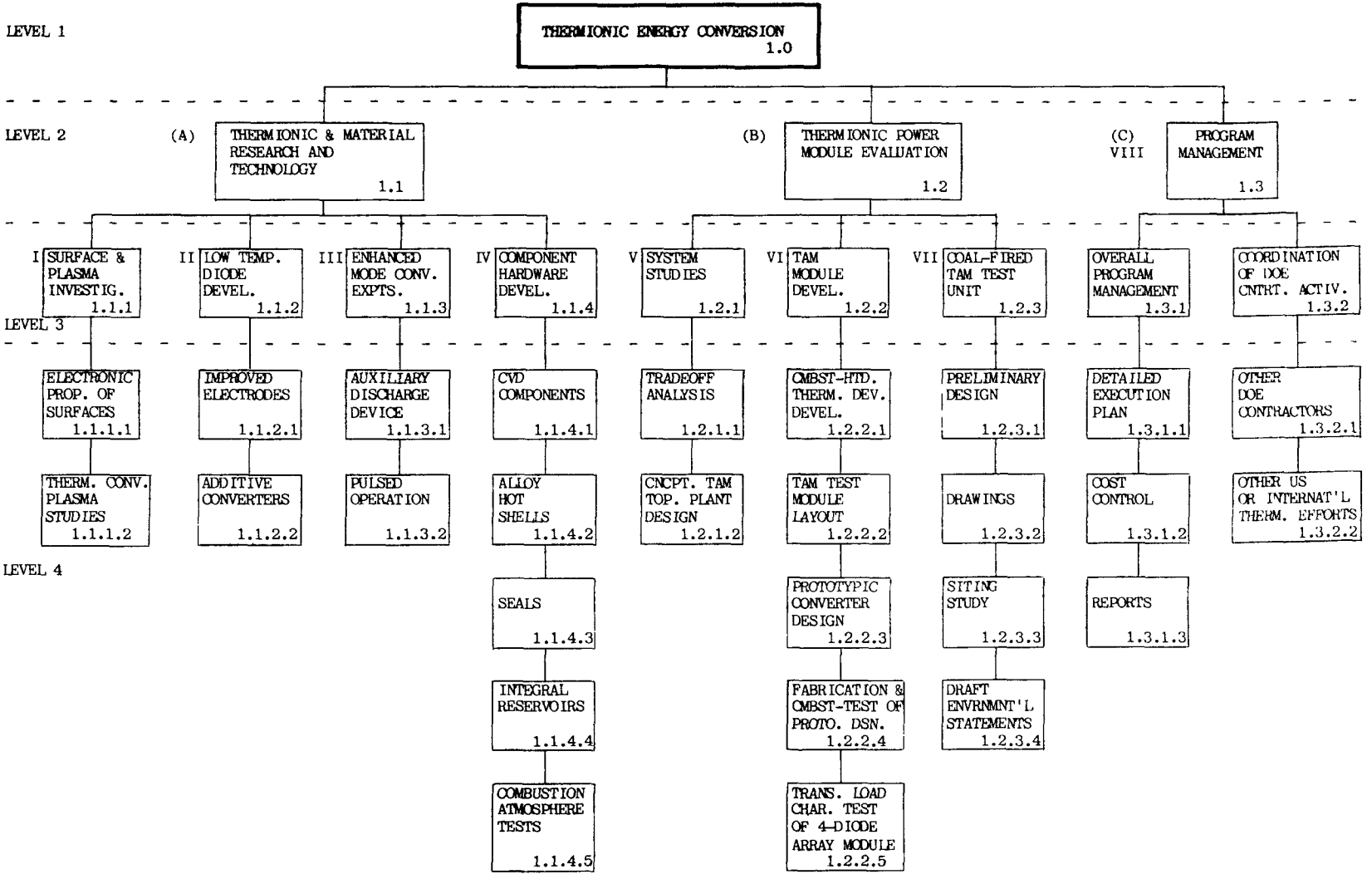


Note: Roman Numerals Designate Level at Which Tasks are to be Reported

# JPL Contract No. 955009
# WORK BREAKDOWN STRUCTURE



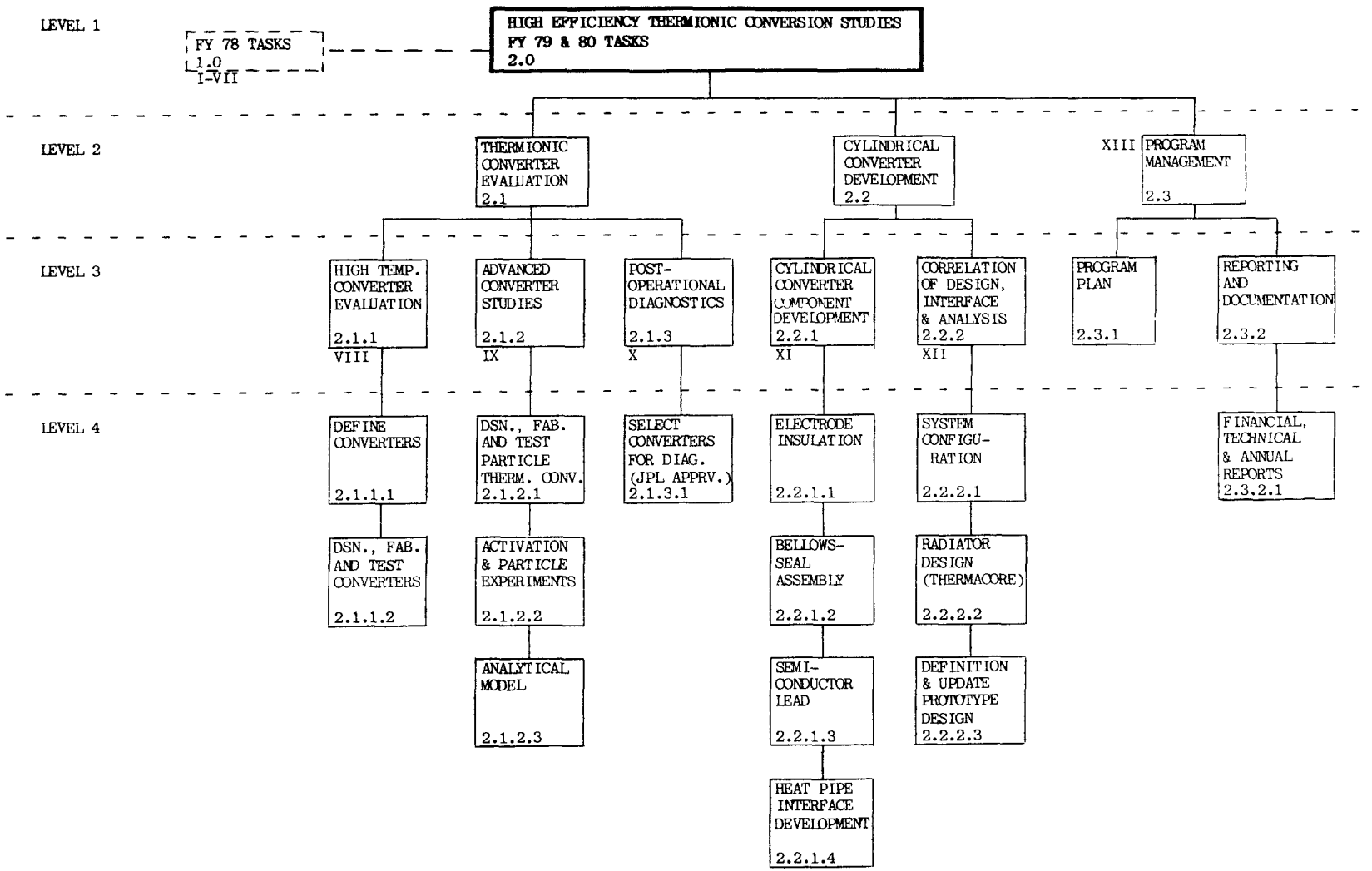


Note. Roman Numerals Designate Level at which Tasks are to be Reported.

# INTRODUCTION AND SUMMARY

The Advanced Thermionic Technology Program at Thermo Electron Corporation is sponsored by the Department of Energy (DOE) and the National Aeronautics and Space Administration (NASA) via the Jet Propulsion Laboratory (JPL).

The primary long-term goal of the DOE effort is to improve TEC performance to the level that thermionic topping of fossil fuel powerplants becomes technically possible and economically attractive. An intermediate goal is to demonstrate an in-boiler thermionic module in the early 1980's. A short-term goal is the demonstration of the reliability of thermionic operation in a combustion environment.

The focus of the JPL program is to develop thermionic conversion technology appropriate for nuclear electric propulsion (NEP) missions. These missions require operation at collector temperatures that are substantially higher than those associated with terrestrial applications.

The DOE and JPL tasks for developing thermionic energy conversion (TEC) are complementary and synergistic. Converter performance improvement is an area in which one agency's program supports the effort of the other.

This report covers progress made during the three-month period from July through September 1980. During this period, significant accomplishments include:

**DOE PROGRAM**

- Continuing combustion life test of the one-inch diameter hemispherical silicon carbide diode (Converter No. 239) at an emitter temperature of 1730 K for a period of over 2200 hours.
- Thermal shock tests of a composite CVD hot shell-emitter structure by heating to 1875 K and quenching with water (10 times) and liquid nitrogen (10 times). Structure was leaktight after both test series.
- Thermal cycle tests of a composite CVD hot shell-emitter structure with heating and cooling periods less than 30 seconds:
  < 900 K to 1875 K (150 times)
  < 900 K to 2025 K (101 times)
- Successful pressure test of composite CVD hot shell-emitter structure to 500 psi for three hours.

**JPL PROGRAM**

- The average minimum barrier index of the last five research diodes built with sublimed molybdenum oxide collectors was 2.0 eV.
- The converters constructed with sublimed molybdenum oxide collectors have activated in a rapid and well defined manner and given favorable output characteristics which are reproducible after a change in operating point.

# 1.0 PART ONE: DOE TASKS

## 1.1 THERMIONIC AND MATERIAL RESEARCH AND TECHNOLOGY

### 1.1.1 TASK I. SURFACE AND PLASMA INVESTIGATIONS

The objective of this task is to support the development of thermionic energy converters by providing experimental data and analyses relating to plasma characteristics and electrode properties.

A guard ring assembly to measure thermionic work functions has been designed and fabricated (see Figure 1). The molybdenum collector provides a small well-defined area for beam current density measurements. The molybdenum guard is electrically connected externally to the collector and insures a uniform field between the sample and collector.

The entire assembly is initially outgassed by electron beam heating it to 1300 K for 5 minutes with the tantalum filament. The assembly is mounted on insulating blocks facing the sample in the surface characterization chamber.

The guard ring assembly was used to measure the thermionic work function of a Zr-O-W(100) emitter. The emitter was made by heating a W(100) crystal to 1800 K for

8010-44

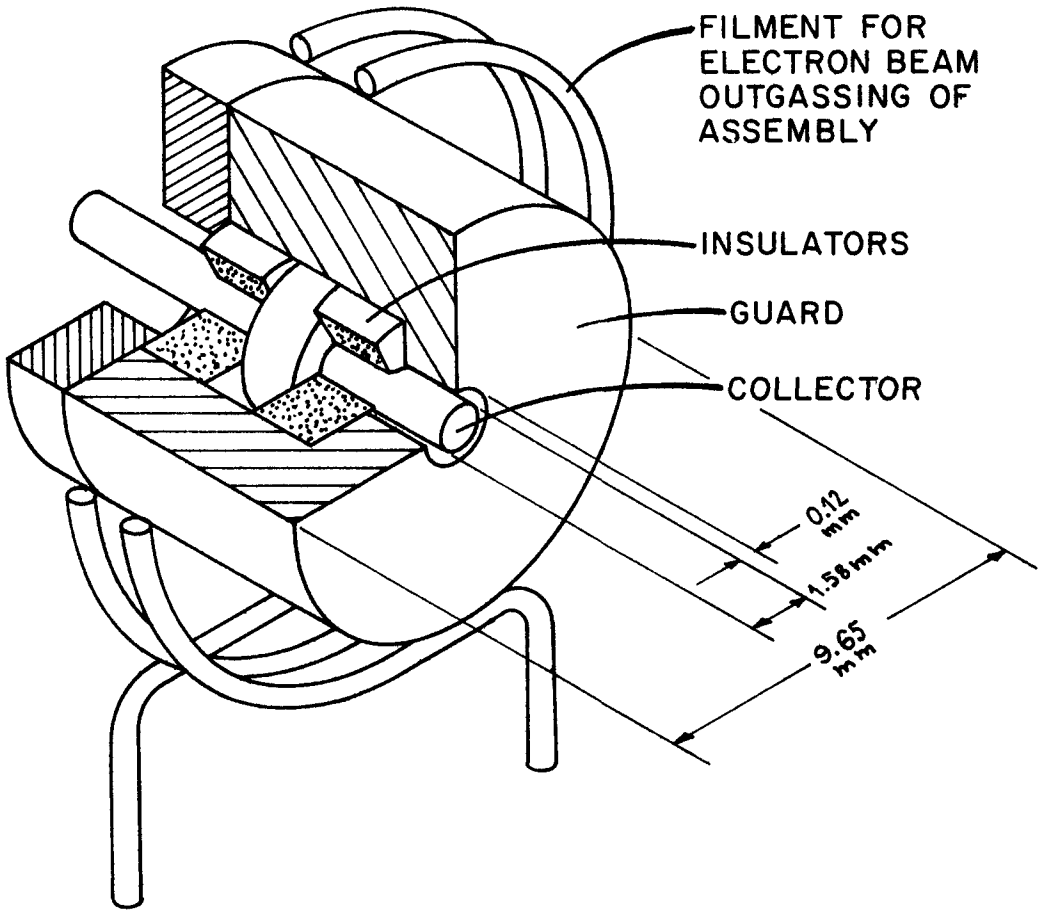


Figure 1. Guard Ring Assembly for Measurement of Thermionic Work Functions

30 minutes during simultaneous zirconium and oxygen doses and then heating to 2100 K in vacuum.

A pulse method for measuring the work function is necessary because of the high currents generated by the DC method which heats the collector. A high voltage pulse with a frequency of 606 Hz and a width of 3 $\mu$sec was applied to the collector and guard while the Zr-O-W(100) emitter was held at ground potential. The emitter was heated from the back by electron bombardment and was rotated to within 1 mm of the guard ring assembly. The emitter temperature was measured with an optical pyrometer and the collector current with a calibrated Tektronix current probe (P6021). The pulse voltage was varied from 200 to 1000 V, and zero field current density values $J_o$ were obtained from extrapolation of Schottky plots (ln J vs V).

A Richardson plot of $\ln(J_o/T^2)$ vs 1/T is shown in Figure 2. Absolute temperatures and current densities are also indicated on the graph. The line is linear from 1450 to 1800 K, which is rather remarkable given the complex nature of the Zr-O-W(100) system. The least squares work function obtained from the slope of this line is 2.54 eV with a pre-exponential $A_R$ value equal to 4. These values

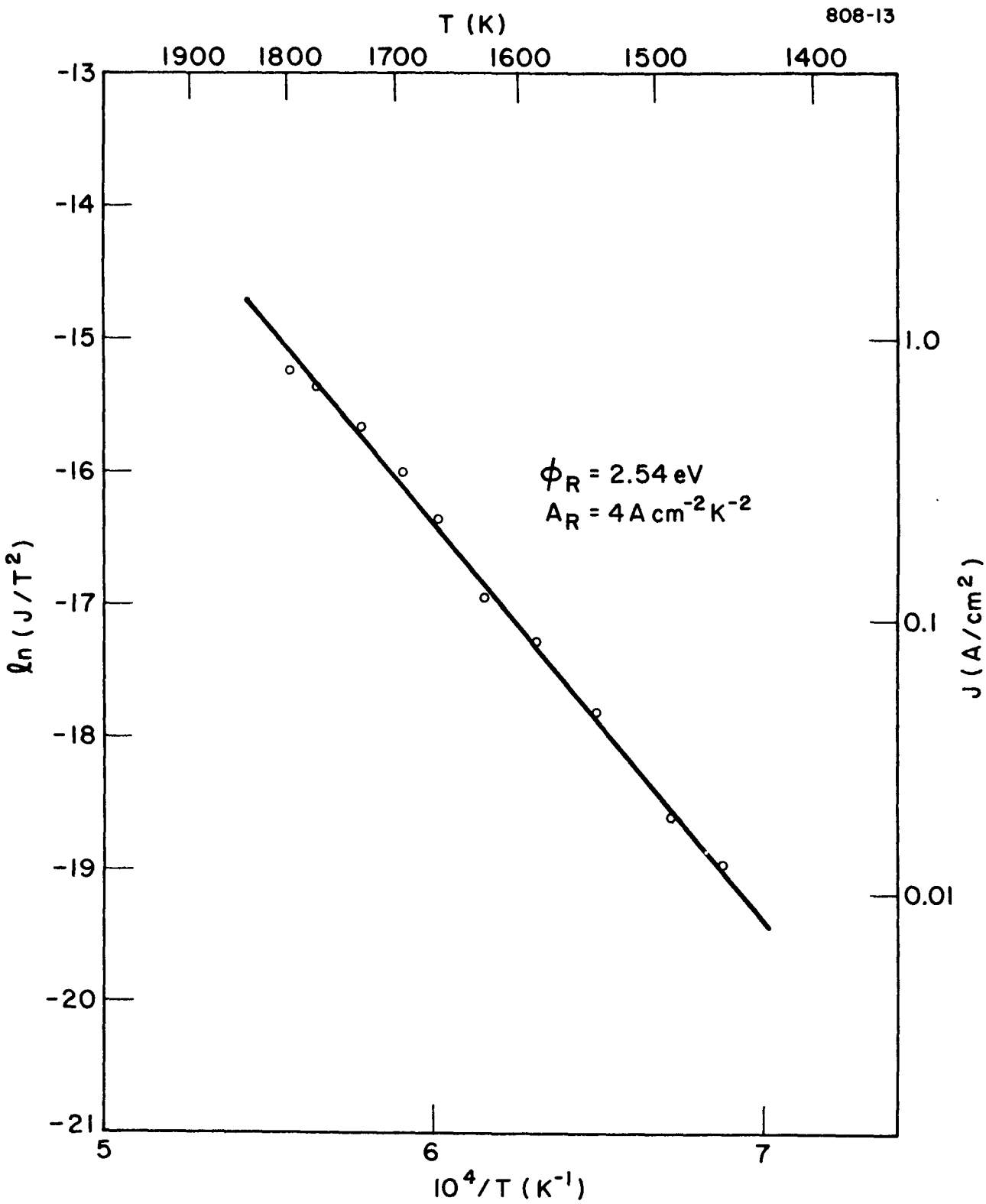


Figure 2. Richardson Plot of $\ln(Jo/T^2)$ vs 1/T For The Zr-O-W(100) Emitter

are in excellent agreement with the thermionic work function of 2.56 eV and $A_R$ = 6 obtained by Danielson and Swanson[1] on a Zr-O-W(100) emitter for temperatures between 1000 and 1450 K. The emitter thus possesses the property of nearly constant work function and $A_R$ value from 1000 to 1800 K.

The low $A_R$ value implies either a very large reflection coefficient or a temperature dependent work function. Theoretically,

$$J_o = 120(1-r)\ T^2 \exp\left(-\frac{\phi_R + \alpha T}{kT}\right)$$

where

r = reflection coefficient

$\phi_R$ = measured Richardson work function

$\alpha$ = constant

Experimentally we measure,

$$J_o = A_R\ T^2 \exp\left(-\frac{\phi_R}{kT}\right)$$

Setting the above two equations equal yields

$$\alpha = k \ln\left[\frac{120\ (1 - r)}{A_R}\right]$$

If we now assume r = 0, we compute $\alpha = 3 \times 10^{-4}$ eV/K. Thus, although the emitter work function of 2.54 eV is

very low, the temperature dependence of the work function causes the effective work function to be much larger. For example, applying $\phi = \phi_R + \alpha T$ for T = 1600 K gives = 3.02 eV. It may be possible to increase the $A_R$ value by a higher bulk dosing of zirconium and oxygen.

A change in elemental surface concentrations with temperature might account for the temperature dependence of the work function. In order to test this hypothesis, a Zr-O-W(100) emitter was heated while facing the Auger spectrometer and the ratios of $Zr_{147}$ to $O_{510}$ peak-to-peak heights were measured as a function of temperature (see Figure 3). The graph shows a relatively constant Zr/O ratio from 1300 to 1600 K with a definite drop in the ratio from 1600 to 1900 K. Also present is some unexplained hysteresis as the temperature is raised and then lowered. These effects also occur for the $Zr_{142}$ peak which is present due to the oxygen. Although it is difficult to explain the temperature dependence of the work function on the basis of these results, the work function change may be related to coverage changes nonlinearly or there may be a structural rearrangement with temperature.

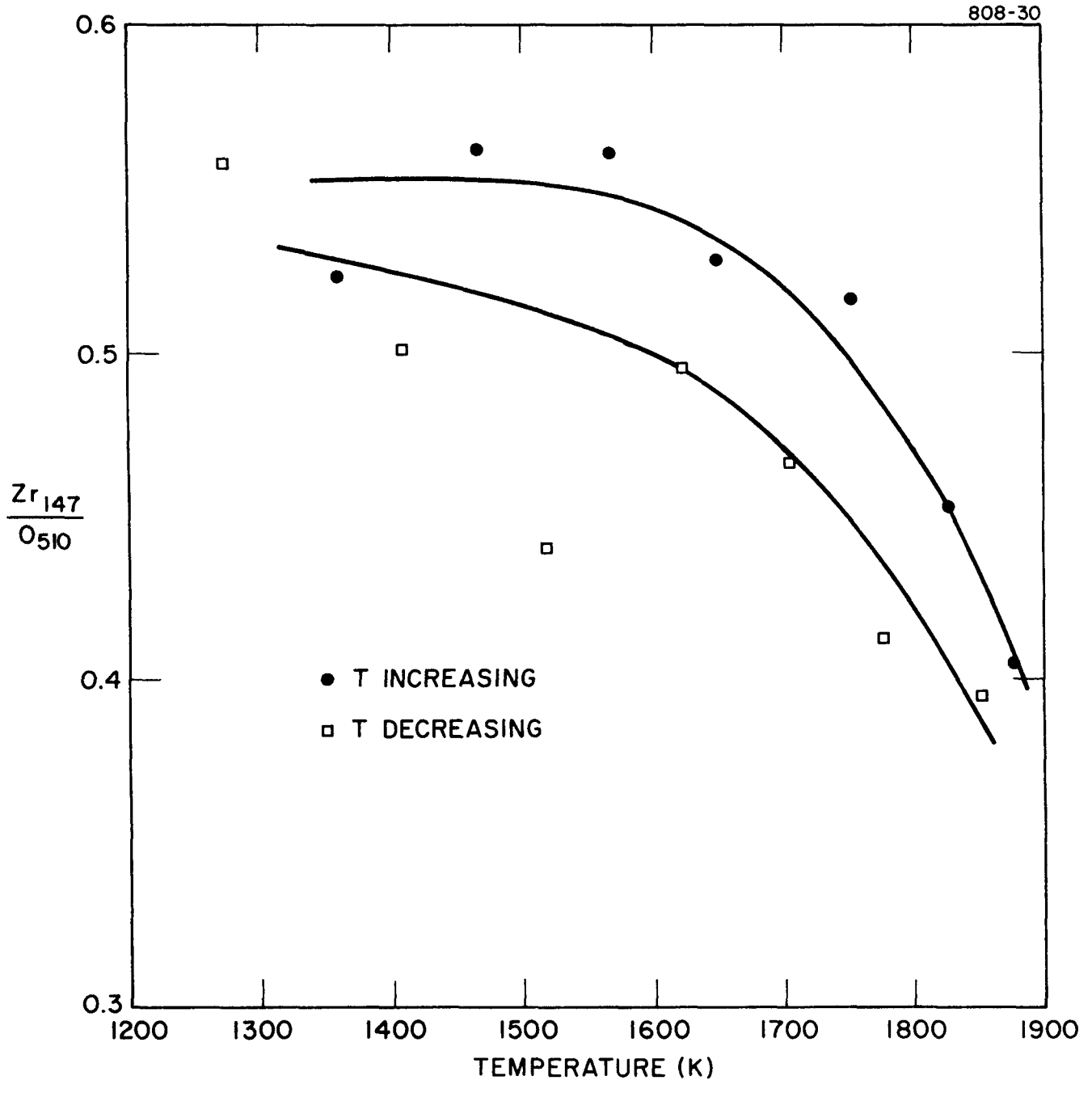


Figure 3. Ratios of $Zr_{147}$ to $O_{510}$ Auger Peak-to-Peak Heights vs Temperature for the Zr-O-W(100) Emitter

Previous work[1] has indicated that the addition of small amounts of carbon to a Zr-O-W(100) emitter can lower the work function. The work functions and percent surface concentrations of a Zr-O-W(100) emitter during heating in CO are shown in Figure 4. The zirconium 92 V Auger peak was used for the concentration calculations for Figures 4 and 5. The emitter was held at 1500 K, the CO pressure was 1 x $10^{-7}$ torr and the measurements were made at room temperature in the absence of CO. The zirconium concentration gradually decreases to 10% of the original concentration and the carbon concentration remains small. The work function rises from 2.80 to 5.0 eV due to the loss of zirconium.

The zirconium concentration can be restored to its original value by heating this CO treated emitter to 2000 K in vacuum, as shown in Figure 5. The concentrations of all other elements also return to their original values before the CO heating. Thus bulk diffusion is the dominant mechanism, similar to the case where a Zr-O-W(100) emitter is heated in oxygen. In the oxygen heating, however, the zirconium disappears into the bulk 60 times faster than with CO.

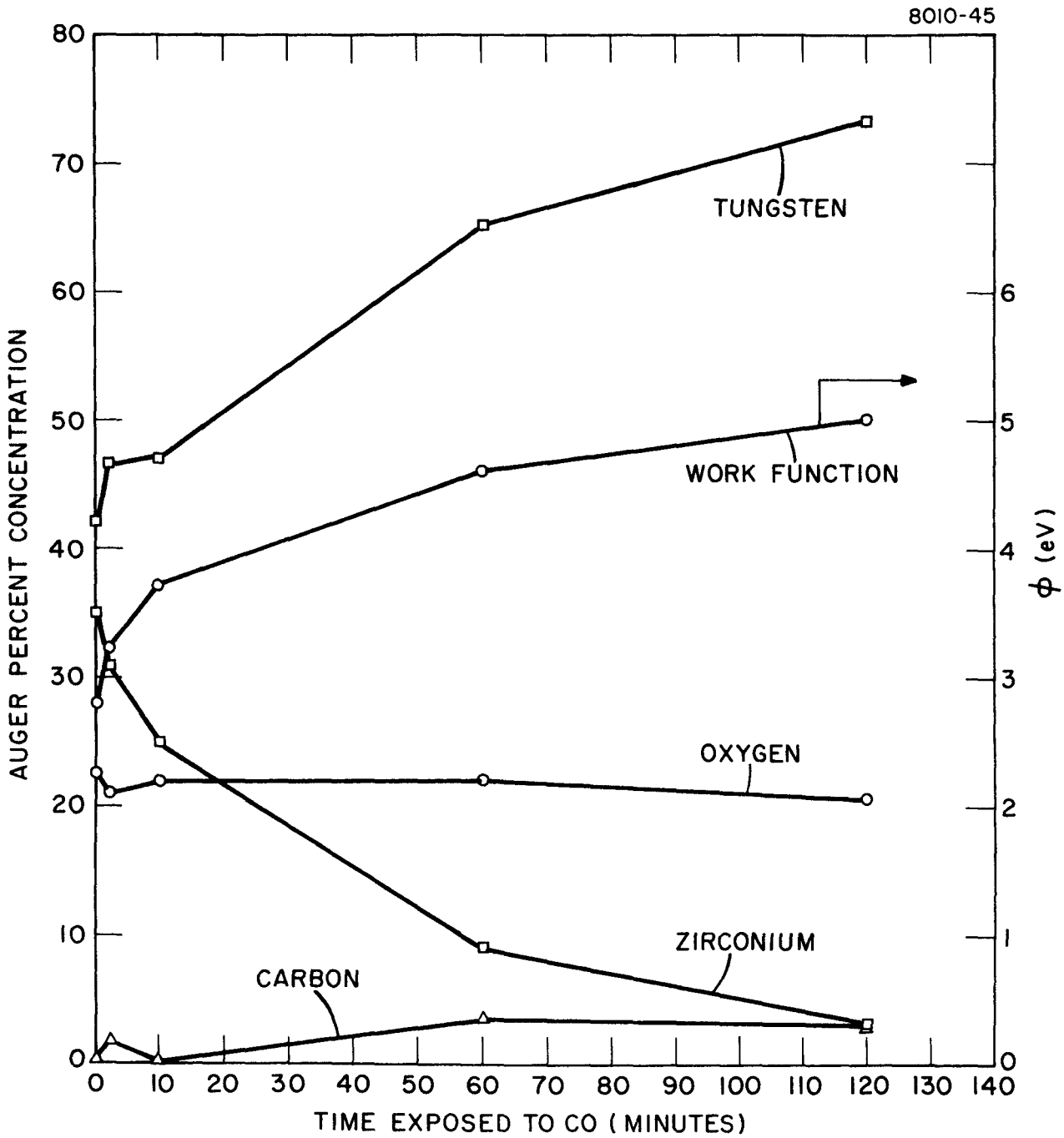


Figure 4. Auger Percent Concentrations and Work Functions vs Time Exposed to CO; P = 1 x $10^{-7}$ torr, T (tungsten) = 1500 K

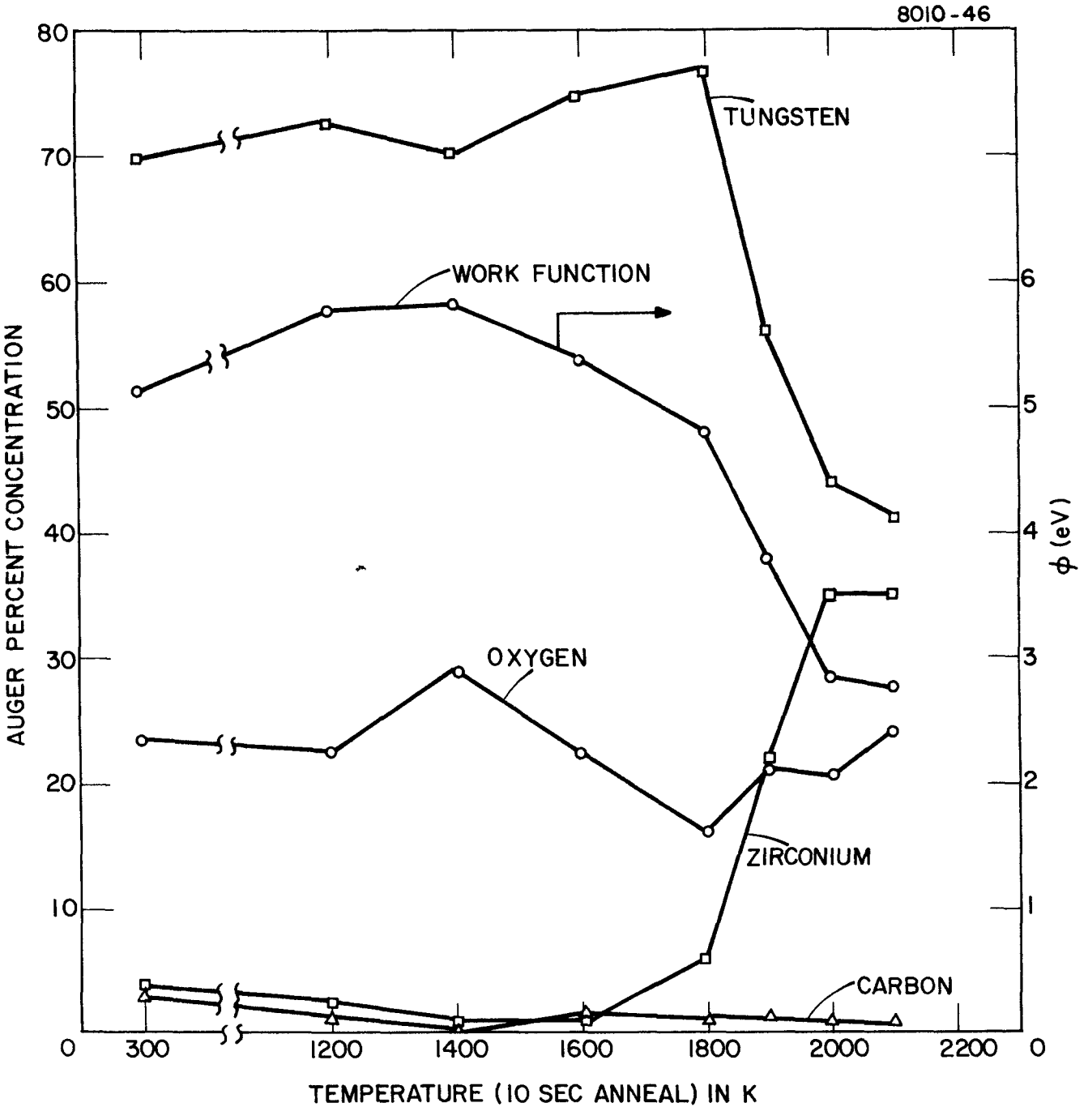


Figure 5. Auger Percent Concentrations and Work Functions vs Anneal Temperature After 2 Hours of Heating in CO

Since the procedures shown in Figure 4 and 5 do not increase the carbon concentration above 3.5 percent, it is necessary to add carbon by a different method. Work is in progress to develop a technique for dosing the Zr-O-W(100) electrode with carbon at higher concentrations in order to obtain a lower work function.

### 1.1.2 TASK II. LOW-TEMPERATURE CONVERTER DEVELOPMENT

The objective of this task is to develop thermionic diodes with improved performance at low collector temperatures (i.e., 500 to 900 K). Converter characteristics will be measured as a function of emitter temperature, collector temperature, cesium pressure, interelectrode spacing and, if applicable, additive gas pressure.

#### A. Converter No. 246: Heat Flux Diode

This diode has a tungsten emitter and a 201 nickel collector. The converter has been thoroughly outgassed to ensure clean, nonoxygenated electrodes.

The current-voltage characteristics are shown in Figure 6 for an emitter temperature of 1400 K, a collector temperature of 750 K, an interelectrode spacing of 0.50 mm and various cesium pressures. The barrier index at a current density of 5 $A/cm^2$ was 2.06 eV at the above conditions. Figure 7 shows a collector temperature family at $T_E$ = 1400 K, $T_R$ = 507 K and d = 0.50 mm. As can be seen from this figure, no appreciable increase in emitter saturation current with increasing collector temperature is discernible. This is an indication that the electrodes are nonoxygenated.

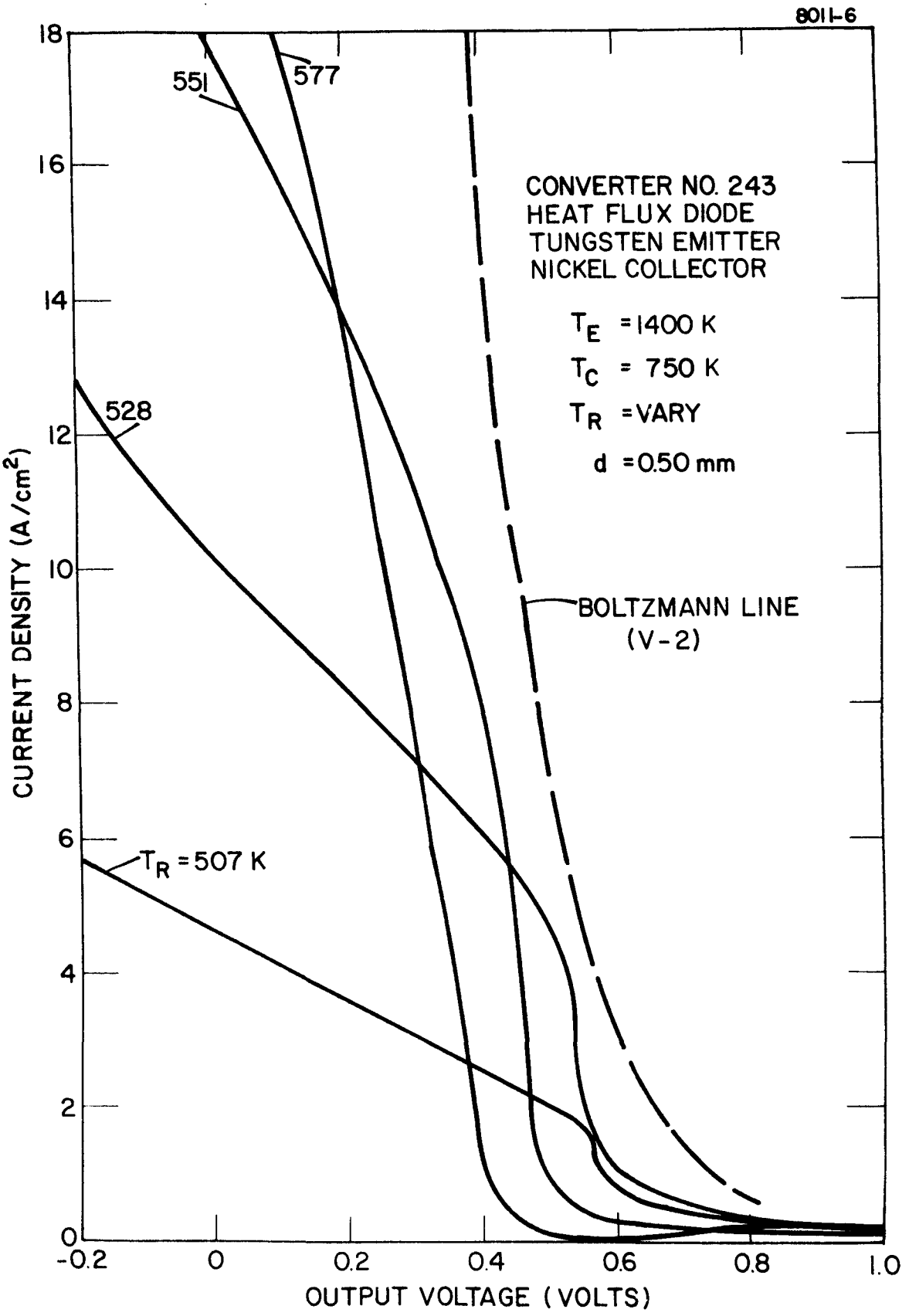


Figure 6. Cesium Reservoir Temperature Family at $T_E$ = 1400 K; $T_C$ = 750 K, and d = 0.50 mm for Converter No. 243

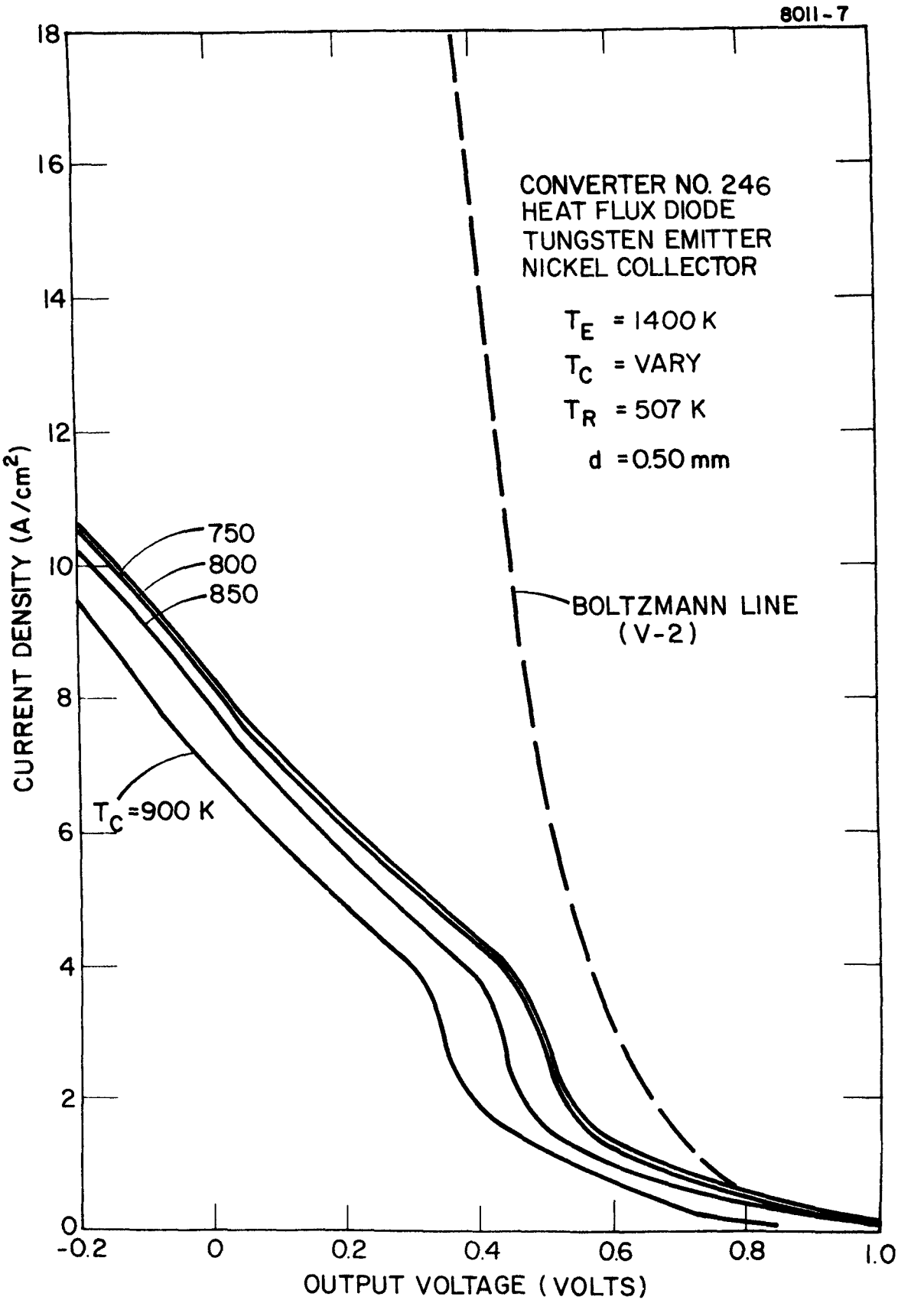


Figure 7. Cesium Reservoir Temperature Family at $T_E$ = 1400 K; $T_C$ = 750 K, and d = 0.50 mm for Converter No. 246

Prior to collector heat flux measurements, the diode will be characterized at various emitter temperatures and the collector work function will be measured by the retarding plot method.

### 1.1.3 TASK III. ENHANCED MODE CONVERTER EXPERIMENTS

The objective of this task is to formulate and evaluate thermionic converter configurations which have the potential of operating more efficiently than the conventional ignited mode diode. In the ignited mode, the mechanism for supplying the ions for space charge neutralization is not efficient. Other techniques that allow the converter to operate in the unignited mode (e.g., those utilizing auxiliary discharge regions and surface contact ionization electrodes) should be more efficient in producing ions and, hence, more efficient in converting heat into electricity. Close-spaced devices that do not require ions should also be more efficient than ignited mode diodes. In the ignited mode, structured electrodes offer the possibility of significantly reducing the plasma losses. Several types of enhanced mode converters will be investigated experimentally.

During this reporting period, effort on this task was limited to an evaluation of magnetic shims as a technique for achieving close spacing in research converters in order to focus program effort on combustion heated diode development.

### 1.1.4 TASK IV. COMPONENT HARDWARE DEVELOPMENT

The objective of this task is to develop converter hardware suitable for operation in a combustion atmosphere such as would be encountered in a thermionic-topped fossil fuel powerplant. Although the effort includes considerable materials evaluation, the focus is on the fabrication and testing of hot shell-emitter subassemblies utilizing chemical vapor deposition (CVD) of composite silicon carbide-graphite-tungsten structures.

#### A. Alloy Hot Shell Development

The testing of alloys in the simulated furnace was concluded. The hot shells were removed for post test analysis.

#### B. CVD Hot Shell-Emitter Development

##### 1) Hot Shell Fabrication

Construction of the three temperature zone Lindberg furnace for CVD of tungsten has been completed (see Figure 8). This furnace will be capable of fabricating structures up to four inches in diameter. All input gases are monitored and controlled by Tylan flowmeters. These meters will

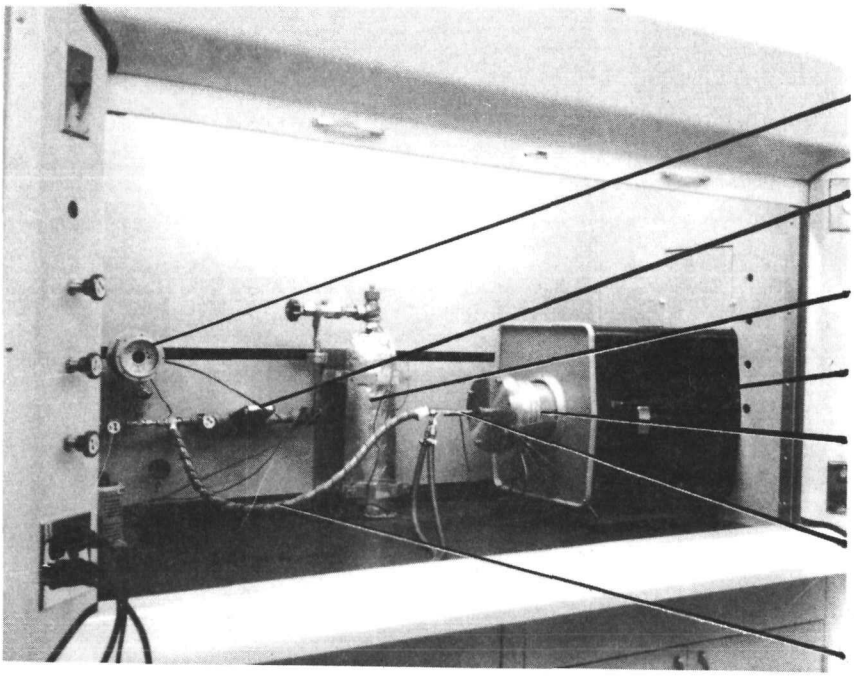


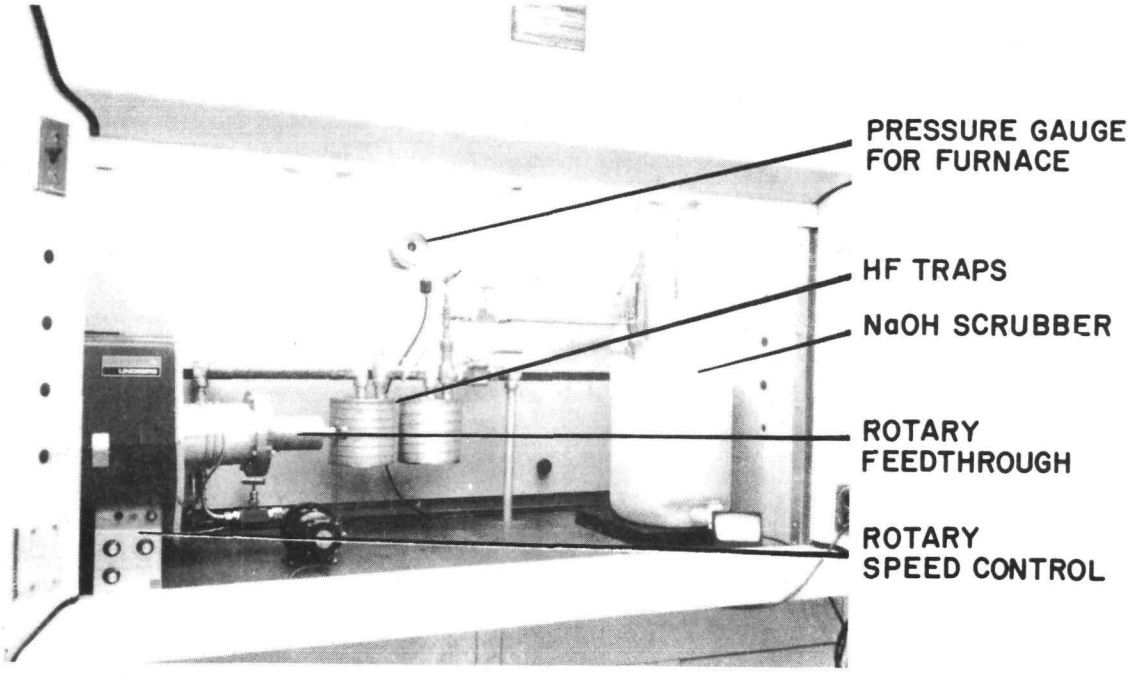


Figure 8. Tungsten Chemical Vapor Deposition (CVD) Apparatus Using Lindberg Furnace

allow precise control of the ratio of tungsten hexafluoride to hydrogen during deposition. Temperature control is within ± 2 C along the hot zone. Four runs were made during this period.

2) Composite Hot Shell-Emitter Flange Life Test Program

Testing at operating temperatures continued on both one- and two-inch diameter hot shell-emitter and flange structures. These shells were heated in air by RF induction or flame fired in a natural gas furnace. The test results are summarized in Table I.

Hot shell-emitter Structure No. 104, which is coated with Cermetal 487 on the flange and braze area, remained leaktight for 2240 hours at an emitter temperature of 1600 K and a flange temperature of 850 K. A crack was observed in the silicon carbide midway between the dome and the flange. The silicon carbide in the region of the crack operated at approximately 1300 K and appears to have reacted with the insulating material surrounding the hot shell. The shell was removed from the furnace after a small rise in pressure was observed. A leak check of the shell showed the dome and braze area to be leaktight.

TABLE I

HOT SHELL-EMITTER-FLANGE STRUCTURE TESTS

| DESCRIPTION (NUMBER) | NUMBER OF HOURS | TEMPERATURE OF DOME OF SHELL | TEMPERATURE OF FLANGE | TEMPERATURE CYCLES | COMMENTS |
|---|---|---|---|---|---|
| 1" DIAMETER 4" LONG SPHERICAL HOT SHELL (101) | 110 | 1925 K | 675 K | 9 | Black residue on flange. No cracking of structure. Tungsten leaktight. |
| 2" DIAMETER 4" LONG SPHERICAL HOT SHELL (102) | 70 | 1655 K | 675 K | 1 | Black residue on flange. SiC cracked and braze swelled. |
| 1" DIAMETER 4" LONG SPHERICAL HOT SHELL (103) | 80 | 1925 K | 850 K | 13 | Flange coated with Cermetal 487. SiC cracked at dome. No black residue. |
| 2" DIAMETER 3" LONG SPHERICAL HOT SHELL (104) | 2480 | 1600 K | 850 K | 10 | Flange coated with Cermetal 487. SiC leaked 1" from nose. Braze area remained leaktight. |
| 1" DIAMETER 4" LONG SPHERICAL HOT SHELL (105) | 70<br>4<br>2 | 1875 K<br>1875 K<br>2025 K | 675 K<br>675 K<br>700 K | 20<br>150<br>100 | Leaktight after 70 hours at 1875 K. Thermal cycles from 900 K to dome temp. Heating and cooling period 30 seconds. |
| 2" DIAMETER 3" LONG SPHERICAL HOT SHELL (107) | 700 | 1600 K | 850 K | 2 | Test Continuing |
| 2" DIAMETER 3" LONG SPHERICAL HOT SHELL (108) | 30 | 1600 K | 850 K | 1 | Test Continuing |

The shell was cross sectioned in order to inspect the braze area (see Figure 9). A small amount of swelling (probably due to oxidized molybdenum) is evident on the outside of the braze area. However, swelling this was observed on the flange after 100 hours of operation and did not increase during the subsequent 2300 hours of the operation. The copper braze was unaffected on the bottom and the inside of the shell.

Two additional two-inch spherical shells are being flame tested at 1600 K on the emitter and 850 K at the flange. Shell No. 107 has silicon carbide nodules on the dome. Occasionally such nodules develop during the CVD of silicon carbide and have been a cause for rejection for converter construction. This is an opportunity to test a shell at operating temperature and observe the effect, if any, of the nodules on its integrity.

3) Thermal Shock Tests

Several tests were performed on Shell No. 105 (one-inch diameter hemispherical) to find how well it would resist thermal shock. In this series of tests, heating was by RF induction in air. A small diffusion pump was connected to the shell to monitor leaktightness. After heating the dome of Shell No. 105 to 1875 K for 70

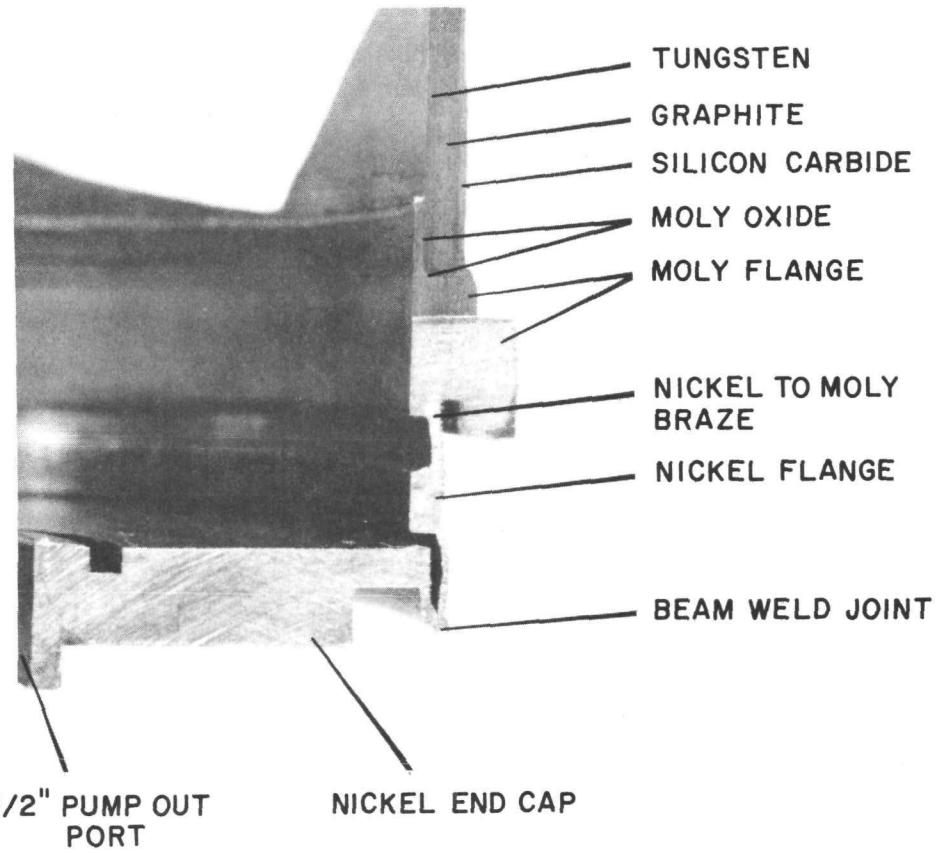


Figure 9. Cross Section of Shell 104 After 2248 Hours of Test in a Gas-Fired Furnace

hours, the shell was still leaktight. The shell was then heated to 1875 K and a water stream was directed to the hottest part of the shell (see Figure 10 a). The area of the shell hit by the water stream turned black within a few seconds while the rest of the dome remained glowing at 1875 K. There was a 1000 K temperature differential between the water cooled spot and the rest of the dome. This test was repeated ten times. A similar series of tests were performed with a quench of liquid nitrogren after the dome was heated to 1875 K (see Figure 10 b). The shell was still leaktight after ten cycles. There was no change in the appearance of the shell.

4) Thermal Cycle Tests

An additional series of thermal cycle tests were performed. The shell was heated in air by RF induction to 1875 K $\pm$ 20 and then cooled to less than 900 K. The heating and cooling times were less 30 seconds. This was accomplished by switching the 10 kW RF power supply full on and off. This shell remained leaktight after 150 cycles.

A similar series of thermal cycle tests were performed with a 50 kW RF power supply. This power supply

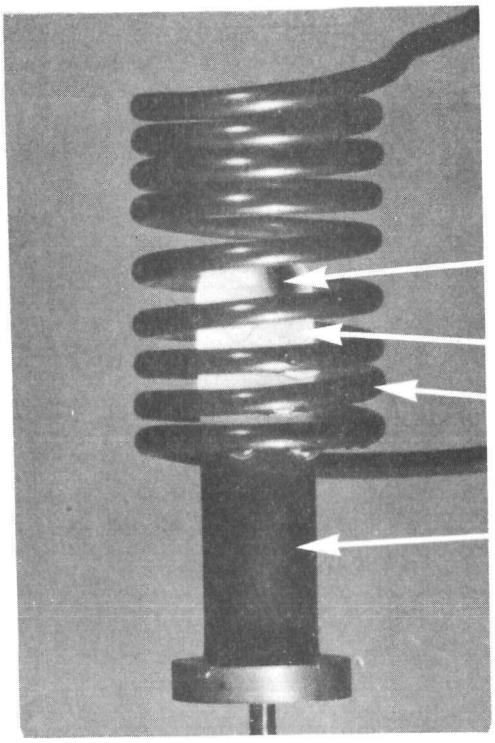


a. Water Quench

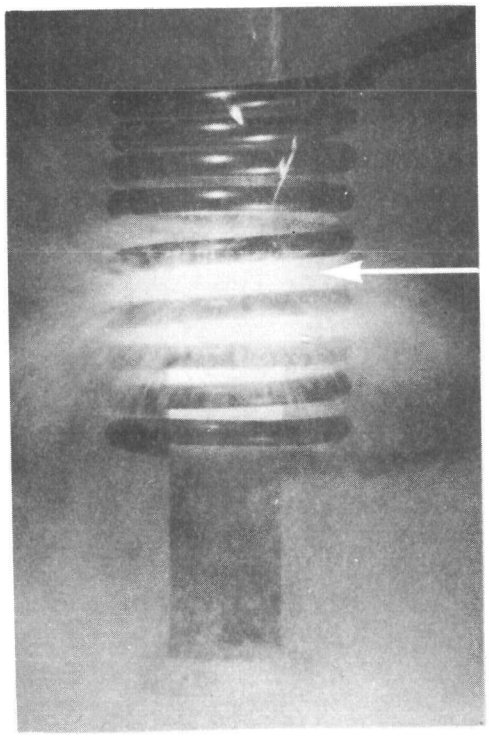


b. Liquid Nitrogen Quench

Figure 10. Thermal Shock Tests With Hot Shell-Emitter Structure Initially Heated to 1875 K in Air

heated the shell in air from less than 900 K to 2025 K in less than 30 seconds. A cooling period of 30 seconds reduced the temperature from 2025 K to less than 900 K. This cycling was repeated 101 times while the pressure on the inside of the shell was constant at $3 \times 10^{-6}$ torr. However, on the next cycle a crack appeared in the CVD silicon carbide near the dome.

5) Hot Shell-Emitter Pressure Test

Application of TAM converters in a pressurized combustor poses the question of the mechanical integrity of the thin-walled CVD composite hot shell-emitter used in the construction of such converters. For example, the TAM Combustor-Combined Cycle System under study in conjunction with Brown Boveri Turbomachinery and Stone & Webster operates at a pressure of ~150 psi. Although published data indicated that silicon carbide had adequate strength for this application, a hardware evaluation appeared desirable. The test arrangement is illustrated in Figure 11. The test specimen was a two-inch diameter hemispherical hot shell-emitter structure with a disk brazed into the open end. This structure was subjected to

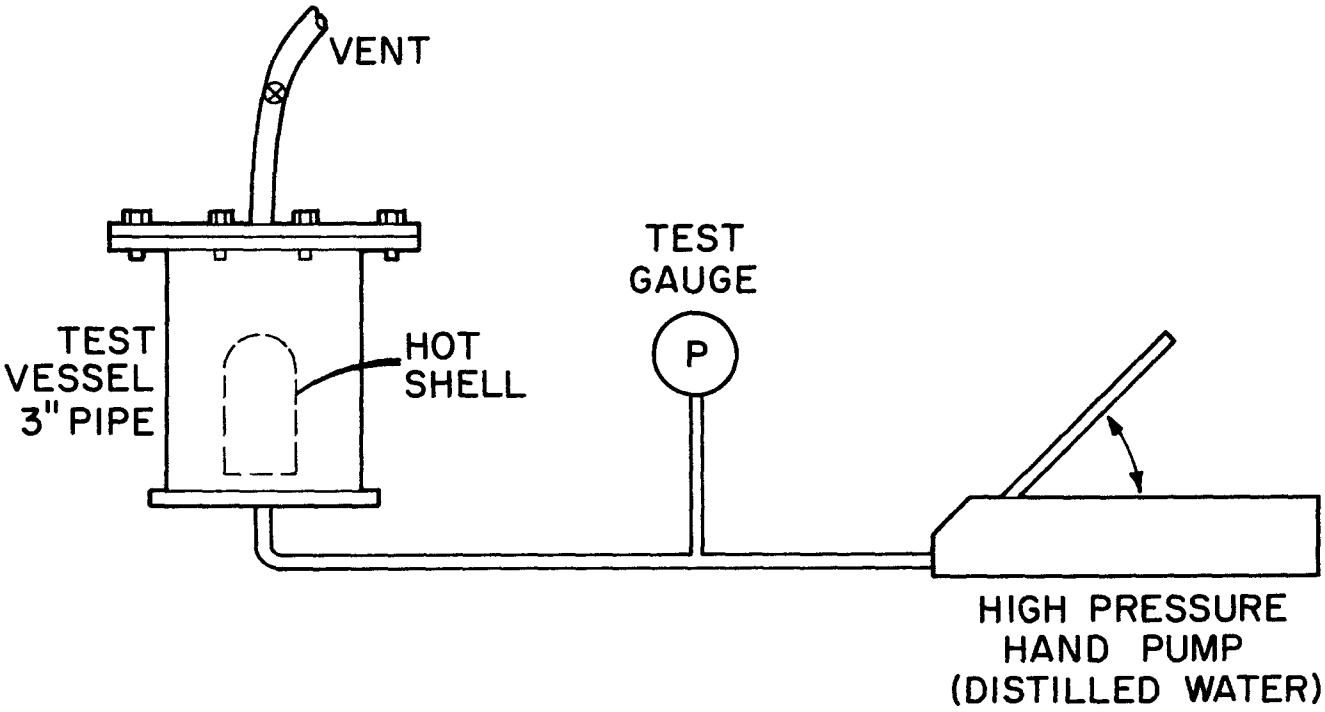


Figure 11. Arrangement of Hot Shell-Emitter Pressure Test

an outside pressure of 500 psi for a period of three hours at room temperature. The unit remained leaktight after this exposure. Although this test was performed at room temperature, the shell integrity is of significance since CVD silicon carbide is almost as strong at 1600 K as it is at room temperature.

## 1.2 THERMIONIC POWER MODULE EVALUATION

### 1.2.1 TASK V. SYSTEM STUDIES

The objective of the system studies task is to identify the design approaches to integrate thermionic energy converters into fossil fuel applications in the most cost effective manner. The results of these studies will help orient the design of the thermionic array module (TAM) being developed in Task VI.

Stone and Webster Engineering Corporation has started the preparation of a topical report on the application of thermionic topping to powerplants. Specific plants studied were a combined gas and steam turbine powerplant and an integrated coal gasifer plant with gas and steam turbines.

### 1.2.2 TASK VI. TAM MODULE DEVELOPMENT

The objective of this task is to develop combustion heated TAM thermionic converters, individually and in small arrays, which are prototypic for topping a central station powerplant. Devices with silicon carbide hot shells will be made and tested. In order to define the transient thermal and electrical characteristics of a TAM, a four-converter array will be constructed and tested.

#### A. Converter No. 239: One-Inch Diameter Hemispherical Silicon Carbide Converter (CVD Tungsten as Deposited Emitter, Nickel Collector)

This converter has been on life test for 2200 hours. During this period, the emitter temperature has been at least 1730 K. The performance throughout the test has remained stable with a barrier index of 2.25 eV and a power output of 2 $W/cm^2$. The life test will continue at the same emitter temperature.

B. Converter No. 247: Two-Inch Diameter Hemispherical Silicon Carbide Converter (CVD Tungsten as Deposited Emitter, Nickel Collector)

This two-inch hemispherical converter was fabricated and tested during the last reporting period. The design of this converter is illustrated in Figure 12. It is similar to that of Converter No. 230 which was damaged during installation. This configuration is much closer to being prototypic than the one-inch diameter hemispherical diodes because the ceramic insulator and the flange are contained almost entirely within the emitter diameter. This design permits the diodes to be closely packed into an array.

The diameter of the emitter is 5 cm and the overall length of the hot shell is 7.6 cm. The active emitter area is 36 $cm^2$. The collector is made from nickel and cooled by passing air through a nickel finned heat exchanger. Both the molybdenum emitter flange and the flange-to-emitter braze were protected from oxidation by coating them with a suspension of silicon carbide.

This converter was outgassed and cesiated before being installed in the multi converter furnace. The hot shell was heated by RF induction to an emitter temperature

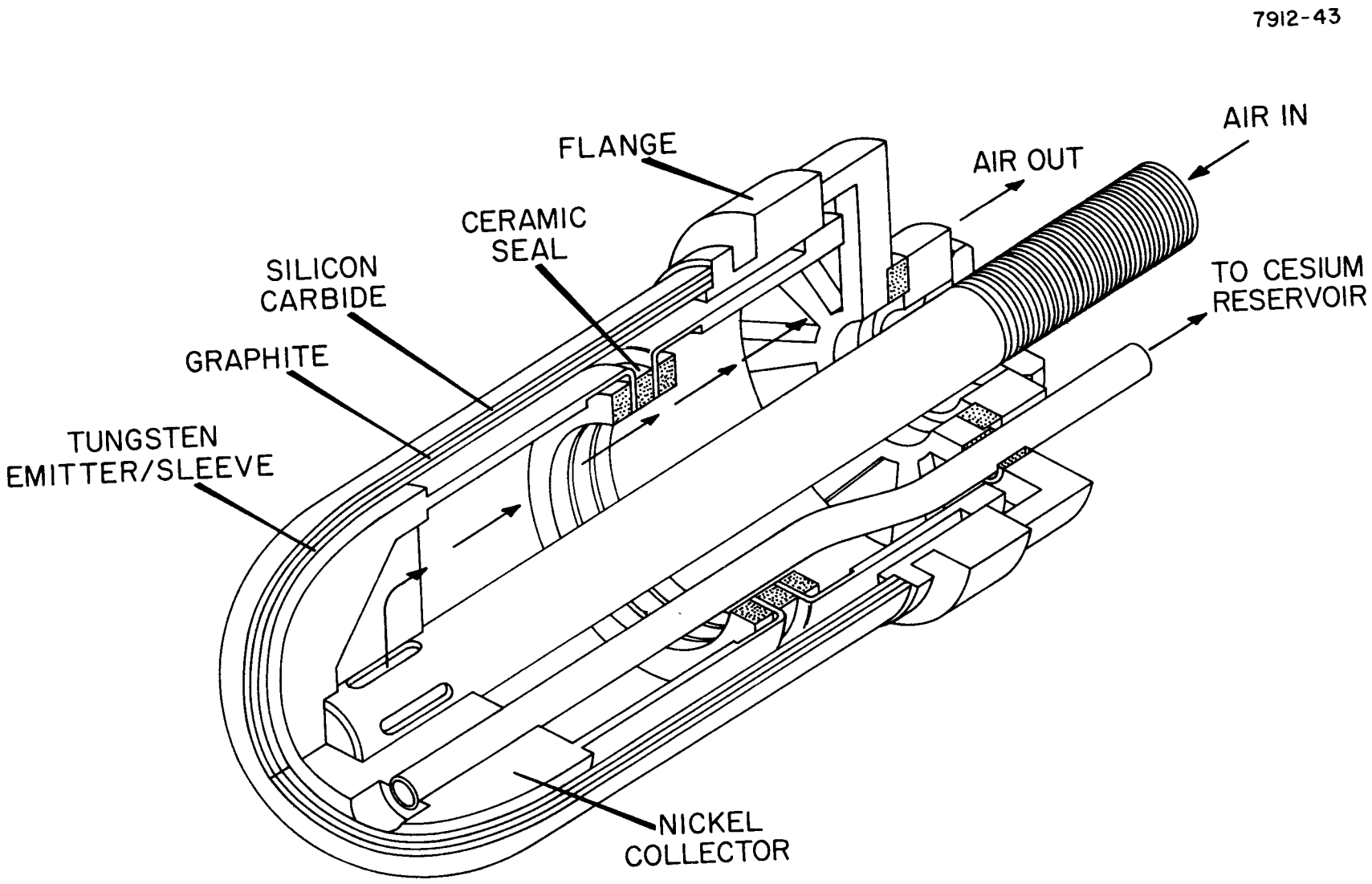


Figure 12. Two-Inch Diameter Hemispherical Silicon Carbide Converter

of 1675 K. The converter pressure at the end of outgassing was less than $10^{-7}$ torr. The cesium reservoir for this converter consists of a nickel tube approximately 15 cm long and 0.5 cm in diameter. The first step in making the cesium reservoir was to machanically pinch off the the copper outgassing tube. Then a nickel pinch off was made on the remaining tubulation with an electron beam welder. The all nickel reservoir eliminates the problem of protecting the copper from oxidation.

The performance data from this converter have not been up to expectation. The barrier index is greater than 2.3 eV. There are two probable causes for this poor performance. First, the temperature over the active area of the emitter varies by as much as 70 K from the tip of the hemisphere to the outer edge. A temperature variation of this degree greatly influences the power output and the barrier index. The value of 2.3 eV is based on the maximum dome temperature. The second problem with this converter is that the spacing between the emitter and collector appears to be larger than optimum. The electrode spacing is fixed during construction and cannot be adjusted during operation.

Converter No. 247, will remain on life test. The converter has operated at an emitter temperature of 1650 K for more than 1100 hours. During this period, the performance has been stable. The hot shell, flange and braze area visually appear to be in excellent condition.

## C. Design of Two-Inch Diameter Torrispherical Silicon Carbide Converter

In order to rectify the spacing and nonuniform temperature problems, a new converter is being designed. The hot shell-emitter configuration will be changed from a hemispherical to torrispherical. This shape has a better view factor to the combustion gases and should heat more evenly. In addition, the torrispherical shape should result in a somewhat lower stress level than the hemispherical. The new design will also include a more positive way of determining and holding the interelectrode spacing. An improved collector heat exchanger is also being designed for this converter.

## D. CVD Silicon Carbide Array Module

During this reporting period, the fabrication of five one-inch diameter hemispherical silicon carbide converters

was begun. Four of these diodes will be mounted in a single fixture which can be readily inserted or removed from the furnace. Initially, the diodes will be connected in electrical series. However, parallel and series-parallel connections can be arranged. The construction of this module is well advanced, and testing is expected to begin during the next reporting period.

### 1.2.3 TASK VII. COAL-FIRED TAM TEST UNIT

The objective of this task is to prepare plans for a TAM coal-fired test unit. The preliminary design will be formulated by taking into consideration the results of the system studies and TAM module development. The TAM test unit design will be the smallest size consistent with a realistic simulation of the temperatures, heat fluxes and slag conditions of a coal-fired steam powerplant.

A visit has been made to Foster Wheeler Development Corporation (FWDC) on 8 July 80 to view a coal-fired test unit and discuss how it could be used to test thermionic energy converters. On the basis of this visit, FWDC is preparing a cost estimate for a coal-fired test unit.

An area of the Thermo Electron Research and Development Center has been identified which would be suitable for such an installation. Discussions with the Massachusetts Department of Environmental Quality Engineering (Air Quality Control) have determined that the FWDC coal-fired test unit would be exempt from air pollution regulations because of its low firing rate. A topical report on siting this unit in Waltham is being prepared.

# 2.0 PART TWO: NASA-OAST/JPL TASKS

## 2.1 THERMIONIC CONVERTER EVALUATION

### 2.1.1 TASK VIII. HIGH-TEMPERATURE CONVERTER EVALUATION

The objective of this task is to characterize the performance of candidate emitters, collectors and converter configurations at the high collector temperatures (900 to 1100 K) required for nuclear electric propulsion. Variable-spaced, planar converters will be used for this task. Evaluation of each converter will include measurements of the output current density versus load voltage as a function of emitter temperature, collector temperature, interelectrode spacing and cesium pressure.

#### A. Converter No. 242 (JPL No. 9): Tungsten Emitter, Molybdenum Oxide Collector

The tungsten emitter of this converter was made by chemical vapor deposition from tungsten hexafluoride. The surface was polished and electroetched to expose 110 facets. The collector was fabricated by subliming molybdenum in the presence of $1 \times 10^{-5}$ torr of oxygen onto a niobium substrate. A sister collector designed at the same time contained 1800 ppm oxygen by weight.

Performance characteristics of this converter were similiar to those of Converter No. 232 (cf. Progress Report No. 42, p. 50). Initially, the converter exhibited a poor barrier index with a somewhat resistive appearance to the current-voltage characteristics. An example of the diode's early performance is given in Figure 13 for $T_E$ = 1650 K; $T_C$ = 750 K; d = 0.50 mm and various cesium reservoir temperatures. After a few hours, the diode output improved dramatically. Figure 13 shows the current-voltage characteristics at $T_E$ = 1650 K; $T_C$ = 800 K; d = 1.00 mm and various cesium reservoir temperatures. A comparison between Figures 13 and 14 show a significant increase in output voltage, a corresponding decrease in barrier index ($V_B$ = 2.06 eV), a decrease in the cesium pressure for a given current density and a corresponding increase in interelectrode spacing. This behavior, like that of Converter No. 232, is a characteristic of an oxygen additive effect.

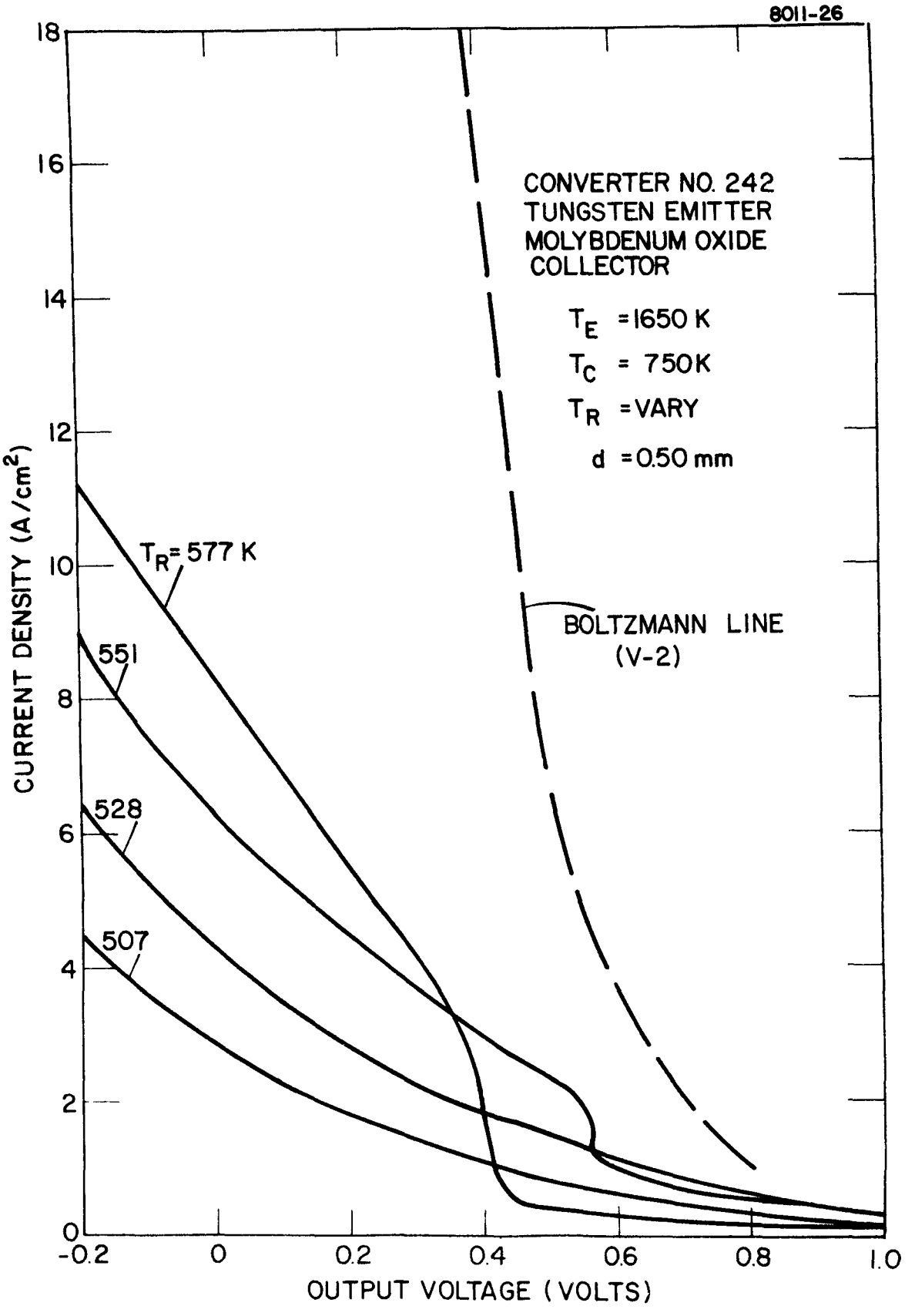


Figure 13. Cesium Reservoir Temperature Family at $T_E$ = 1650 K; $T_C$ = 750 K; d = 0.50 mm for Converter No. 242

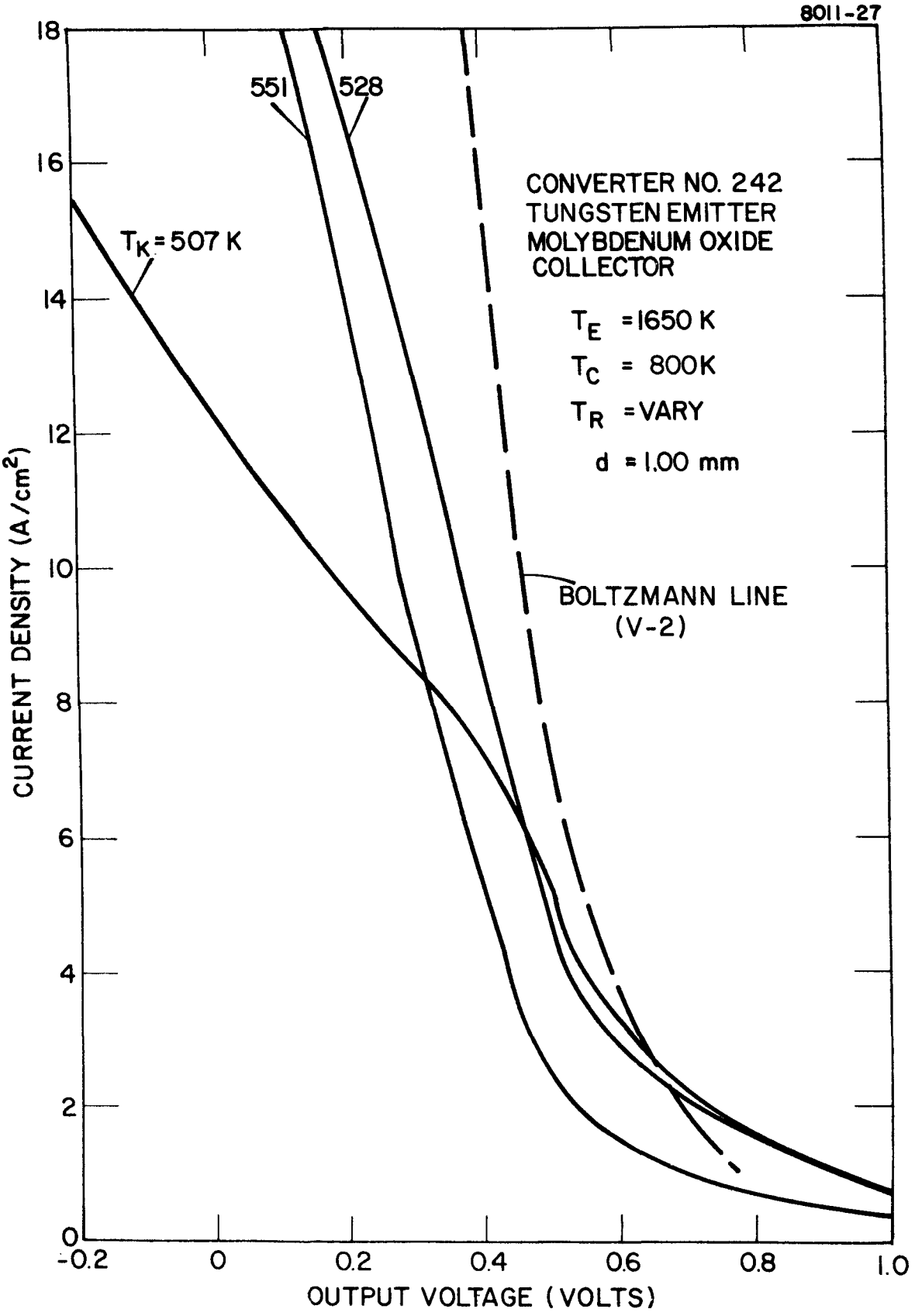


Figure 14. Cesium Reservoir Temperature Family at $T_E$ = 1650 K; $T_C$ = 800 K; d = 1.00 mm for Converter No. 242

The converter was optimized for interelectrode spacing, cesium pressure, and collector temperature at an emitter temperature of 1650 K. The results are given in Figure 15. At a current density of 5 $A/cm^2$, the barrier index was 2.06 eV. In addition, the diode was optimized for cesium pressure and spacing at $T_E$ = 1650 K and collector temperatures of 800, 850, 900, 950 and 1000 K. These results are given in Figure 16.

After the initial improvement, the performance of this diode remained stable throughout the entire testing procedure. It was decided to mount the converter in an ion pumped life test station to evaluate the stability of this electrode pair for a longer period. This test should be started during the next reporting period.

## B. Converter No. 240 (JPL No. 10): Tungsten Emitter, Molybdenum Oxide Collector

This converter is identical in construction to Converter No. 242. The emitter is electroetched CVD fluoride tungsten and the collector is sublimed molybdenum oxide. The collector contained 1800 ppm oxygen by weight.

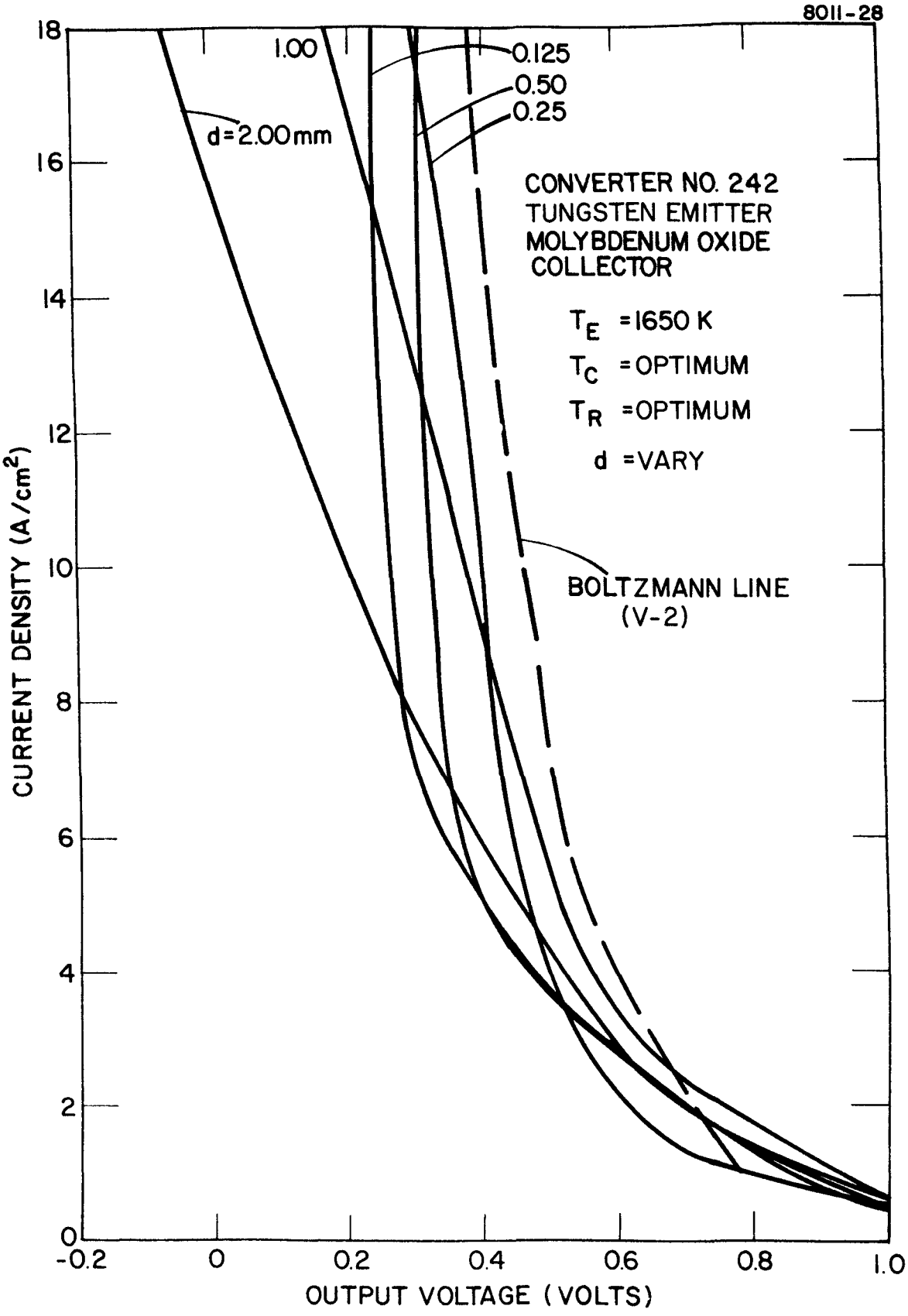


Figure 15. Optimized Converter Performance at $T_E$ = 1650 K

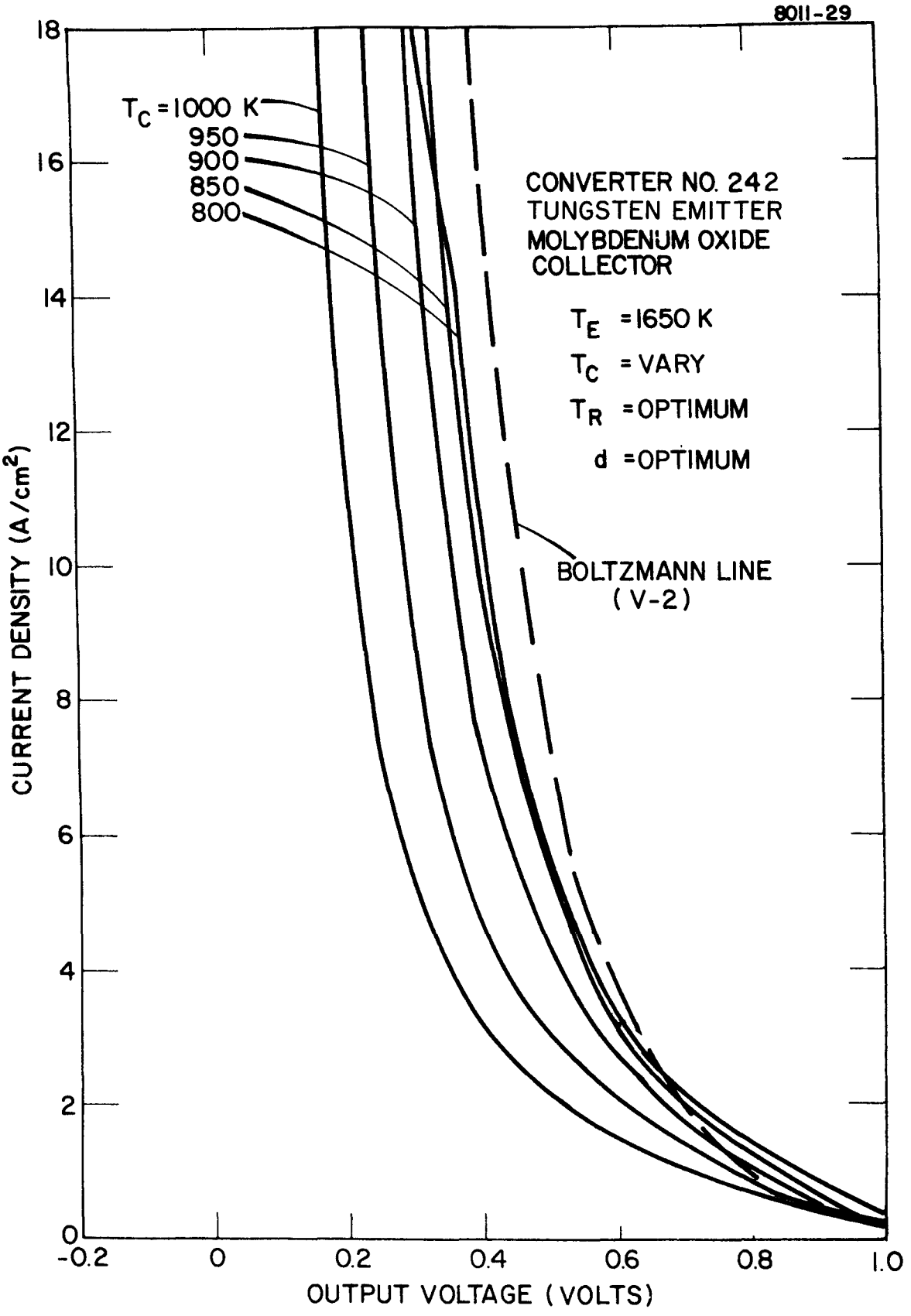


Figure 16. Optimized Converter Performance (Cesium Pressure and Interelectrode Spacing) at $T_E$ = 1650 K and Various Collector Temperatures for Converter No. 242

Initial current-voltage characteristics where resistive and exhibited a large barrier index. Figure 17 shows a cesium reservoir temperature family taken early in the diode's history at $T_E$ = 1650 K, $T_C$ = 800 K and d = 0.50 mm. After a period of about 8 hours, the output voltage increased and the cesium pressure requirements decreased, signaling the onset of the oxygen additive effect. An example of this mode of operation is given in Figure 18 at $T_E$ = 1650 K, $T_C$ = 800 K, d = 0.50 mm and various cesium reservoir temperatures. At this time, the diode was optimized for collector temperature, cesium pressure, and interelectrode spacing at $T_E$ = 1650 K. The optimized curves at these conditions are displayed in Figure 19. At a current density of 5 $A/cm^2$, the barrier index was 2.01 eV. The collector work function was measured by the retarding plot method. The work function is plotted versus the ratio $T_C/T_R$ in Figure 20. The minimum work function of 1.54 eV corresponds to a $T_C/T_R$ of 1.42. In addition, the converter was optimized for cesium pressure and interelectrode spacing at $T_E$ = 1650 K and collector temperatures of 800, 850, 900, 950 and 1000 K. These results are shown in Figure 21.

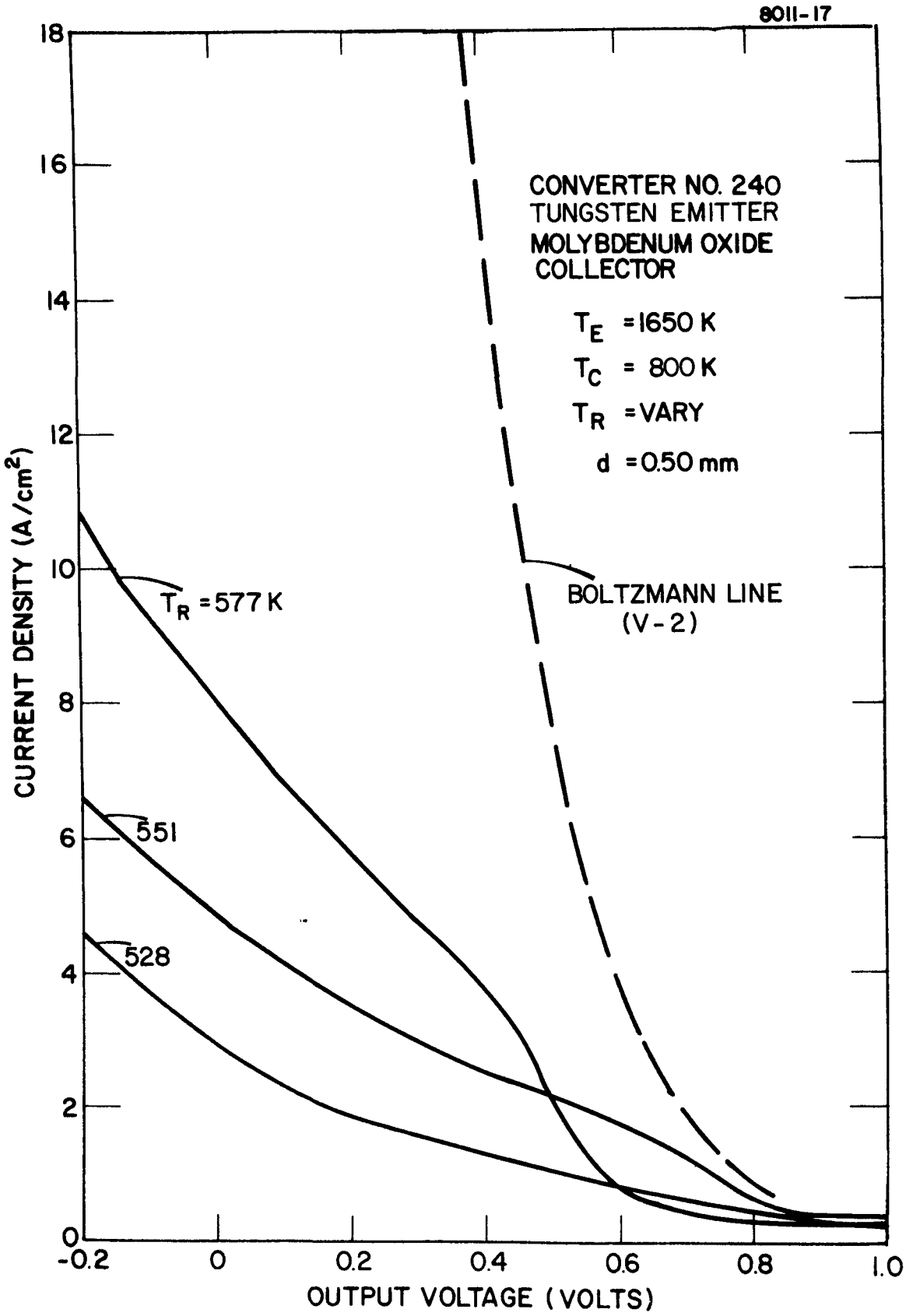


Figure 17. Cesium Reservoir Temperature Family at $T_E$ = 1650 K; $T_C$ = 800 K; d = 0.50 mm for Converter No. 240

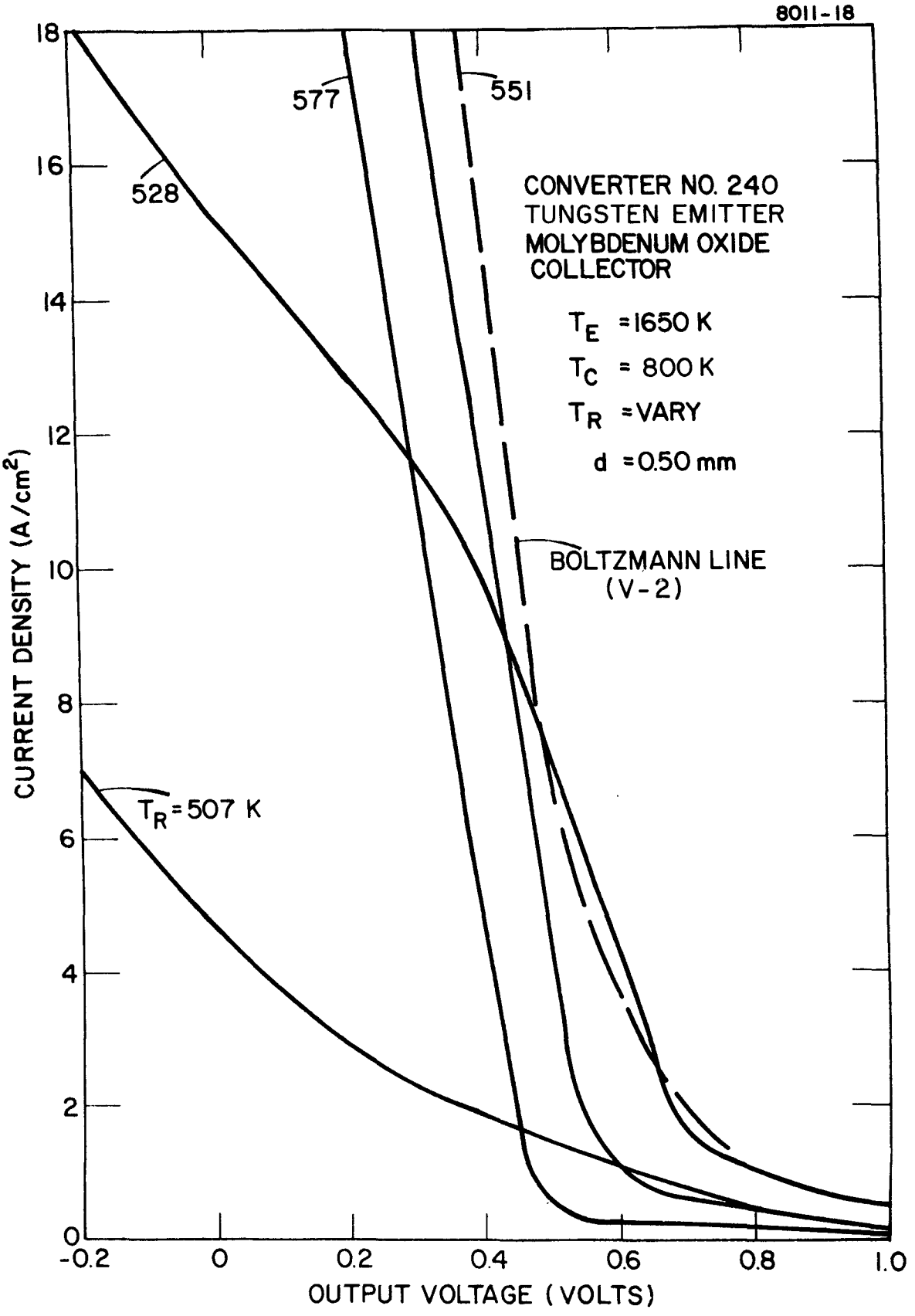


Figure 18. Cesium Reservoir Temperature Family at $T_E$ = 1650 K; $T_C$ = 800 K; d = 0.50 mm for Converter No. 240

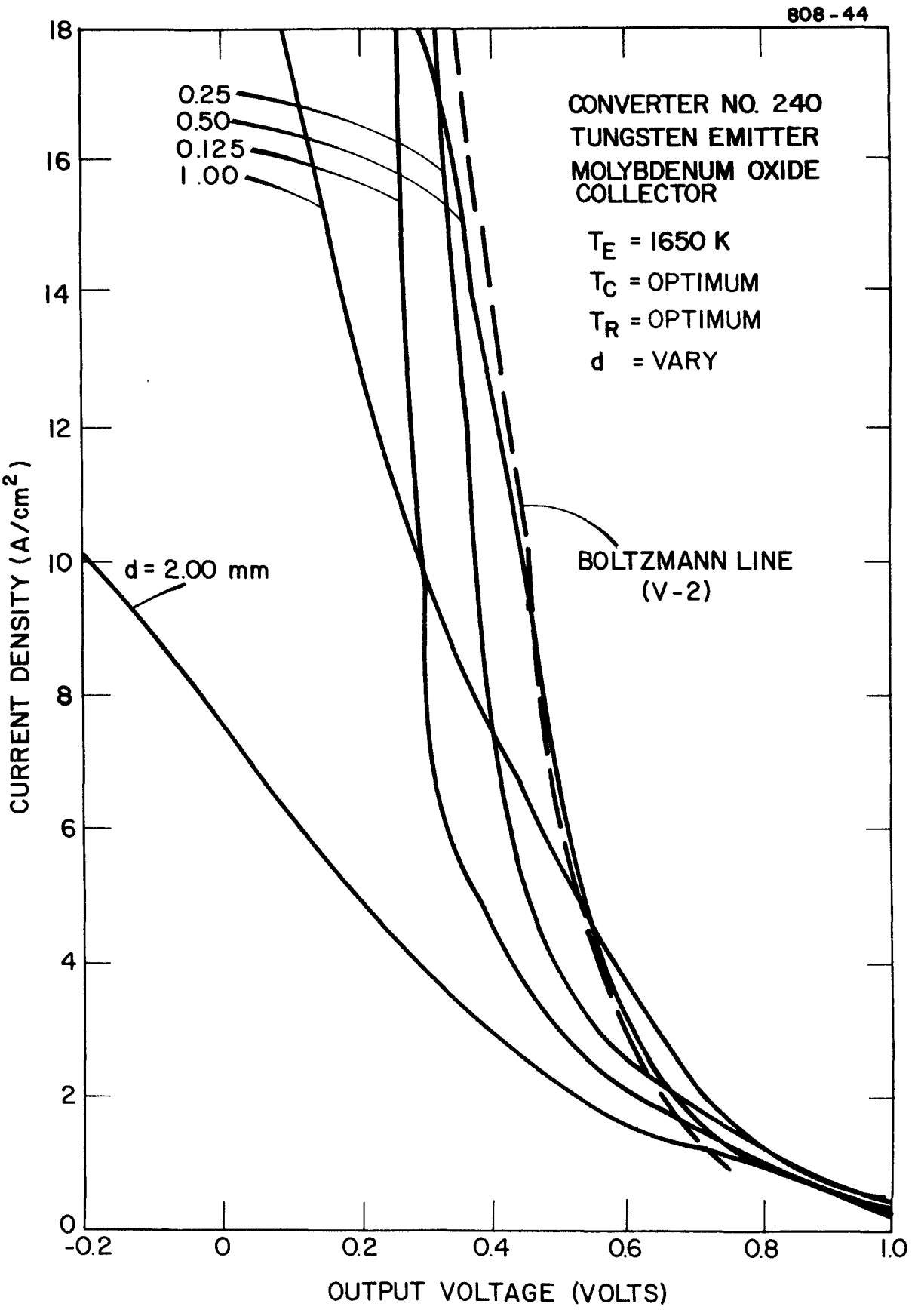


Figure 19. Optimized Performance at $T_E$ = 1650 K at Various Interelectrode Spacings for Converter No. 240

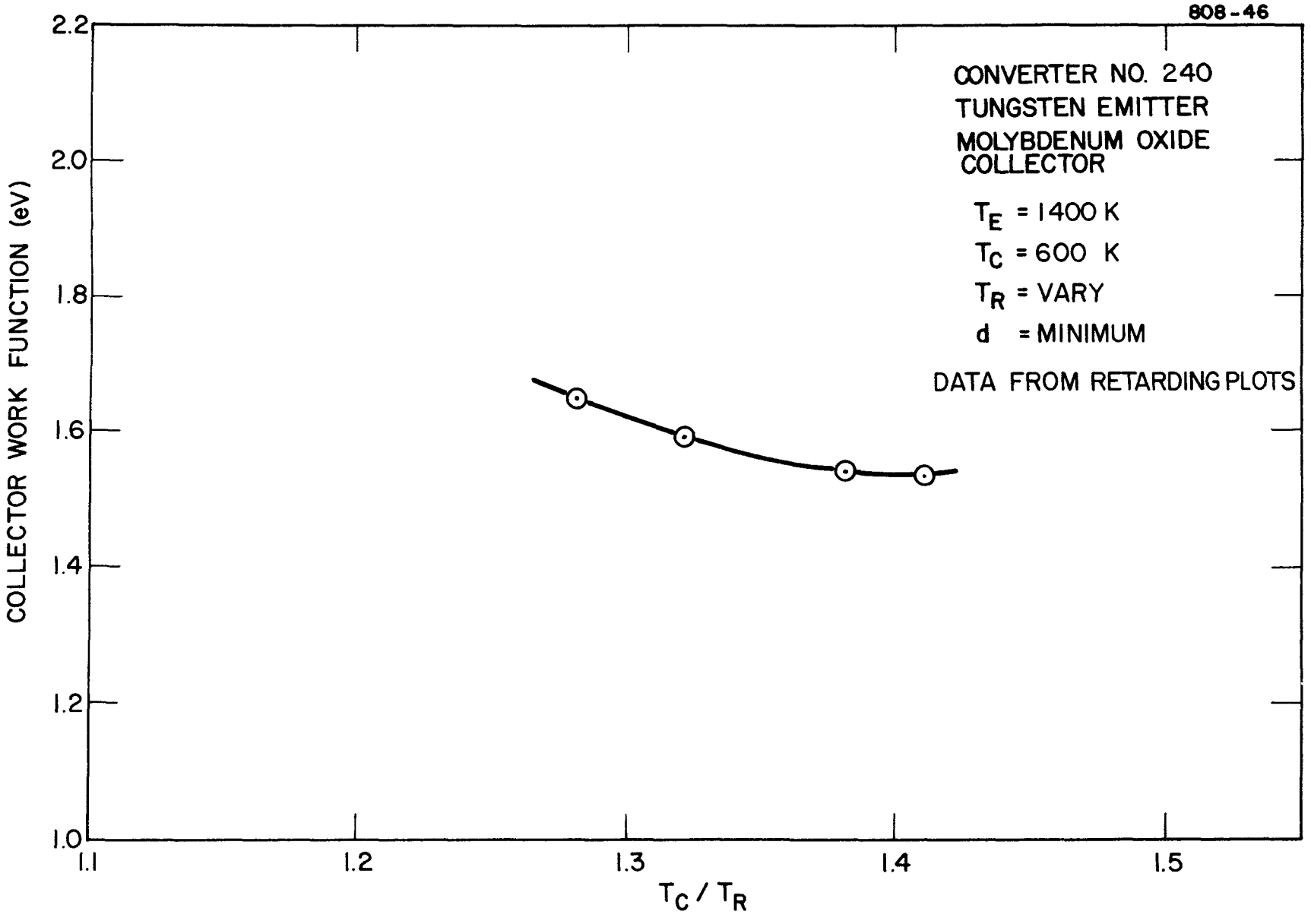


Figure 20. Collector Work Function Versus $T_C/T_R$ for Converter No. 240

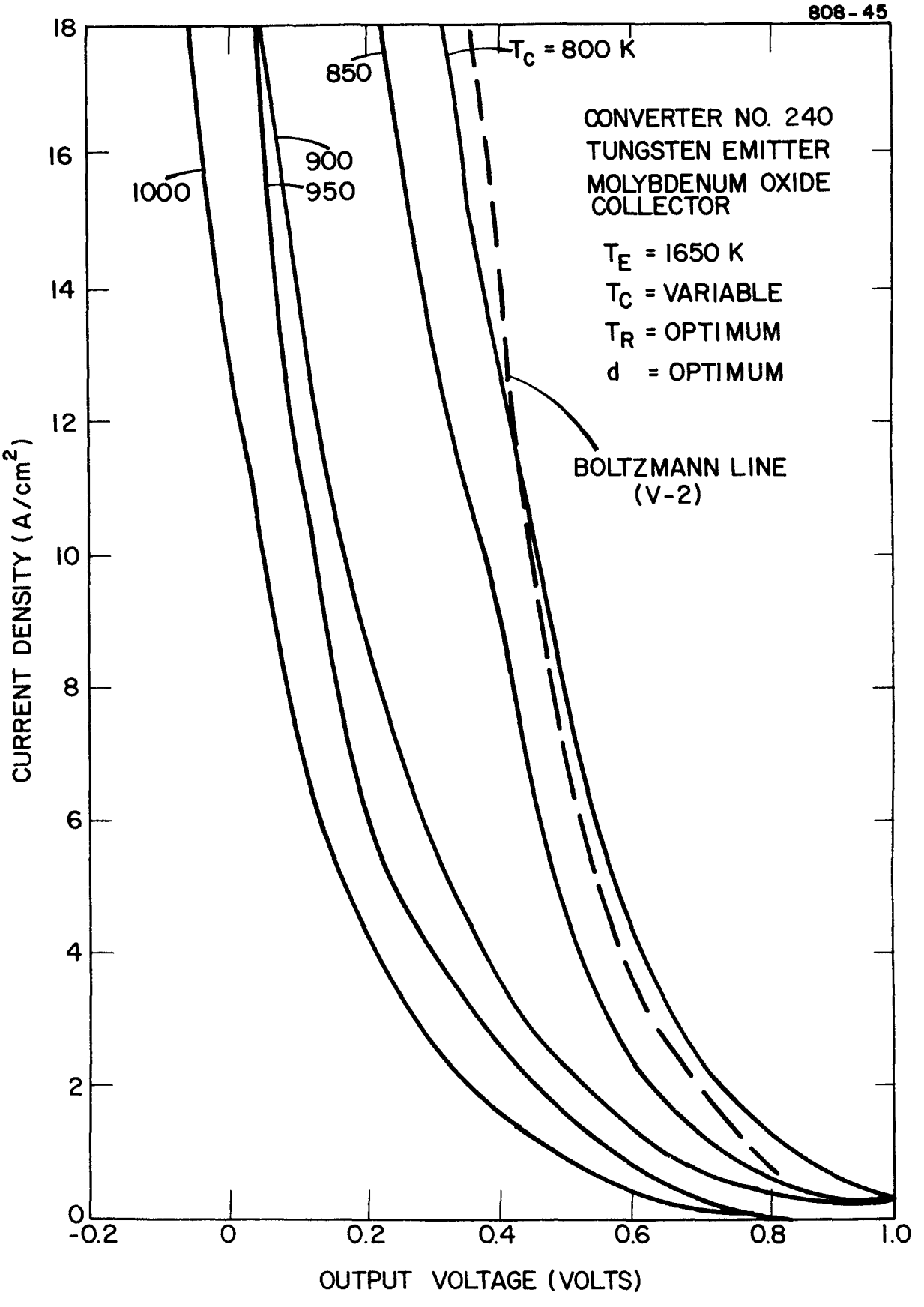


Figure 21. Optimized Performance (Spalling and Cesium Pressure) of Converter No. 240 at $T_E$ = 1650 K and Various Collector Temperatures

After approximately 100 hours of operation, the barrier index increased from 2.01 eV to 2.18 eV. Usually, this behavior is associated with a leak which contaminates the electrodes. During the next reporting period, the diode will be removed from the test stand, dissassembled and leak-checked.

C. Converter No. 241 (JPL No. 11): Tungsten Emitter, Molybdenum Oxide Collector

The emitter of this converter is an as deposited CVD fluoride tungsten. The molybdenum oxide collector contains 18,000 ppm oxygen by weight. This is the highest oxygen content collector produced to date.

As with the last three converters with molybdenum oxide collectors, this diode initially appeared to be non-oxygenated. The barrier index was in excess of 2.20 eV, the J-V curves were resistive and the short circuit current density at $P_{Cs}$ = 0.25 torr was only 5 A/cm$^2$. In less than one hour of operation the enhancement of the output due to the oxygen additive effect occurred. The barrier index decreased to 1.98 eV, and at $P_{Cs}$ = 0.25

torr, the short circuit current density grew to 11 $A/cm^2$. Figure 22 is a cesium pressure family taken before the performance improvement while the data in Figure 23, at identical conditions, was taken afterwards. A comparison of the two figures is a succinct description of the oxygen additive effect.

After approximately 10 hours of operation, an electrical short was observed at an interelectrode spacing of 0.50 mm. The shorting was due to the delamination of the molybdenum oxide collector. Testing was terminated and the diode was leak checked. No leak was found. After disassembly of the diode, inspection showed that the debonding was not at the niobium-molybdenum interface, but at the molybdenum-molybdenum oxide interface. Diagnostic results on the collector of this converter are given in Section 2.1.3 of this report.

Evidence from this converter and Converter No. 243 (see Section D) suggest that with the present method of molybdenum oxide deposition, debonding of the oxide layer is likely when oxygen concentrations are in excess of 15,000 ppm.

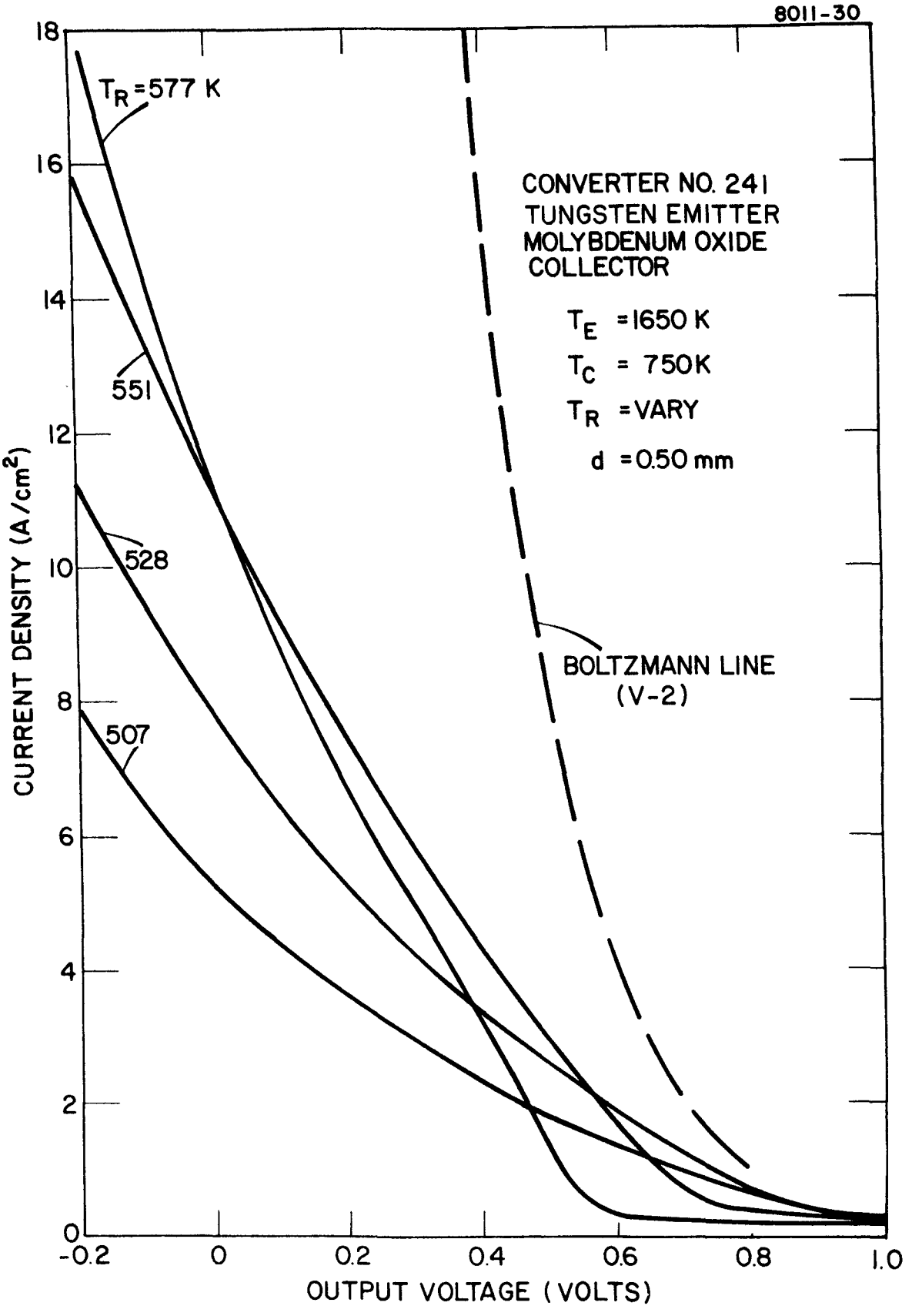


Figure 22. Cesium Reservoir Temperature Family at $T_E$ = 1650 K; $T_C$ = 750 K; and d = 0.50 mm for Converter No. 241

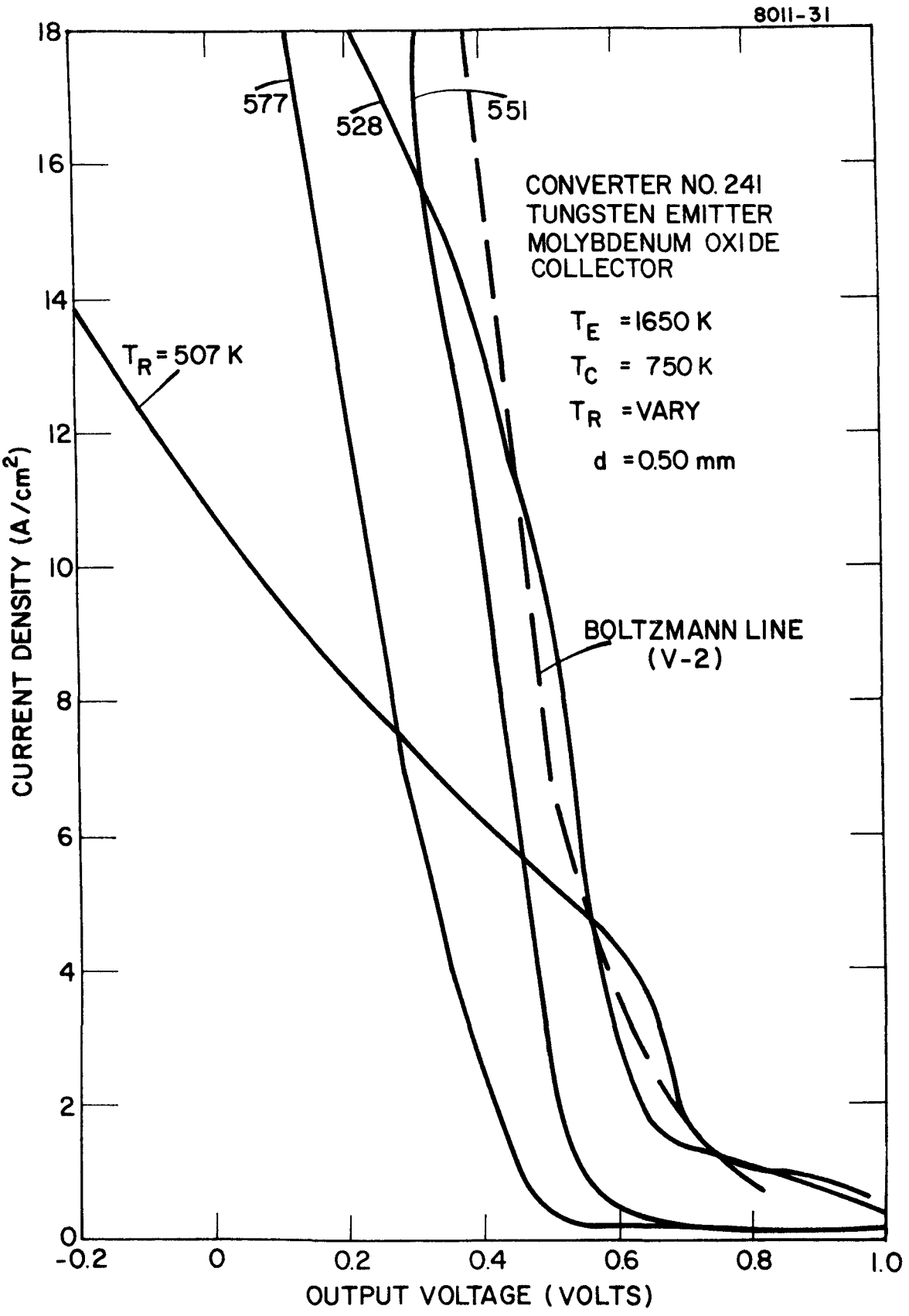


Figure 23. Cesium Reservoir Temperature Family at $T_E$ = 1650 K; $T_C$ = 750 K; d = 0.50 mm for Converter No. 241

Enough evidence is now available to postulate a modus operandi for converters containing molybdenum oxide collectors. Converter Nos. 232, 240, 241 and 242 initially exhibited poor barrier indices and resistive current--voltage characteristics. The high cesium pressure requirements and the corresponding close spacing suggest nonoxygenated electrodes. Within a short period of operation, typically between 2 and 20 hours, performance improves dramatically. The barrier index decreases to approximately 2.0 eV and the J-V curves lose their resistive character. In addition, high current densities can be obtained with low cesium pressures which, in turn, allow greater interelectrode spacing.

The above behavior is attributed to an oxygen additive effect. In addition to reducing the collector work function, it appears that an oxide whose source is the collector is made available to increase the current density from the emitter for a given cesium pressure and emitter temperature. Experiments detailed in the previous progress report (cf. Progress Report No. 43, p. 45) indicate that a cesium oxide is the species transported to the emitter. The microprobe analysis of the collector from Converter No. 241 supports this conclusion. After

operating in a cesium atmosphere for several hours, the oxide coating was found to be porous with a quasi-uniform distribution of cesium and oxygen throughout the layer. However, molybdenum oxide coatings containing concentrations as high as 28,000 ppm oxygen have been thermally cycled in vacuum with no observable effects. It appears that cesium interacts with the resistive molybdenum-molybdenum oxide coating to produce a more conductive layer which supplies a volatile cesium oxide to the emitter.

D. Converter No. 243 (JPL No. 12): Rhenium Emitter, Molybdenum Oxide Collector

This diode has an as-deposited CVD rhenium emitter. An SEM of the rhenium surface is shown in Figure 24. The molybdenum oxide collector, sublimed in the same run as the collector for Converter No. 241, contained 18,000 ppm oxygen by weight.

After a brief testing period, problems of delamination of the molybdenum oxide coating were encountered. Upon dissassembly, it was apparent that the collector coating had expanded appreciably. Large portions of the oxide layer had flaked from the collector.

8011-32

X1000

Figure 24. SEM of the As Deposited CVD Rhenium Emitter for Converter No. 243

The debonding was at the molybdenum-molybdenum oxide interface. It appears that cesium reacts with the molybdenum oxide layer to produce a molybdenum-cesium oxide layer. The associated expansion, exacerbated by the high oxygen concentration, is probably the cause of debonding.

Apparently, there is no effect of oxygen on the rhenium emitter. However, a number of observations suggest the presence of oxygen in the diode. The experience gained in operating a number of diodes containing molybdenum oxide collectors shows this type of collector surface to be a ready source of oxygen for an emitter. In fact, this diode's sister collector (sublimed at the same time and also containing 18,000 ppm oxygen) was installed in Converter No. 241 opposite a tungsten emitter. In that diode, the oxygen additive effect was pronounced, and it occurred within an hour of the introduction of cesium (see Section C). Moreover, the debonding of this collector coating suggests that the chemical changes which are responsible for making oxygen available to the emitter had taken place. The relatively low barrier index of this converter ($V_B$ = 2.06 eV) also suggests a low collector work function in addition to a highly conductive surface which seems to be concomitant with the oxygen additive

effect. However, no lowering of the emitter cesium requirement was observed. A cesium reservoir temperature family is shown in Figure 25 at $T_E$ = 1650 K, $T_C$ = 750 K and d = 0.50 mm. The cesium pressures in this diode are comparable to those in Converter No. 48, which contained a rhenium emitter and a niobium collector. Figure 26 is a cesium reservoir temperature family at $T_E$ = 1600 K, $T_C$ = 723 K and d = 0.21 mm for Converter No. 48.

The behavior of the rhenium emitter in Converter No. 243 is similar to that of a diode with an iridium emitter and tungsten oxide collector which also did not show an additive oxygen effect. Both rhenium and iridium are noted for their high bare work functions. Although the data available are too limited to make a firm generalization, they suggest that additive oxygen effects may not be observed with high bare work function emitters.

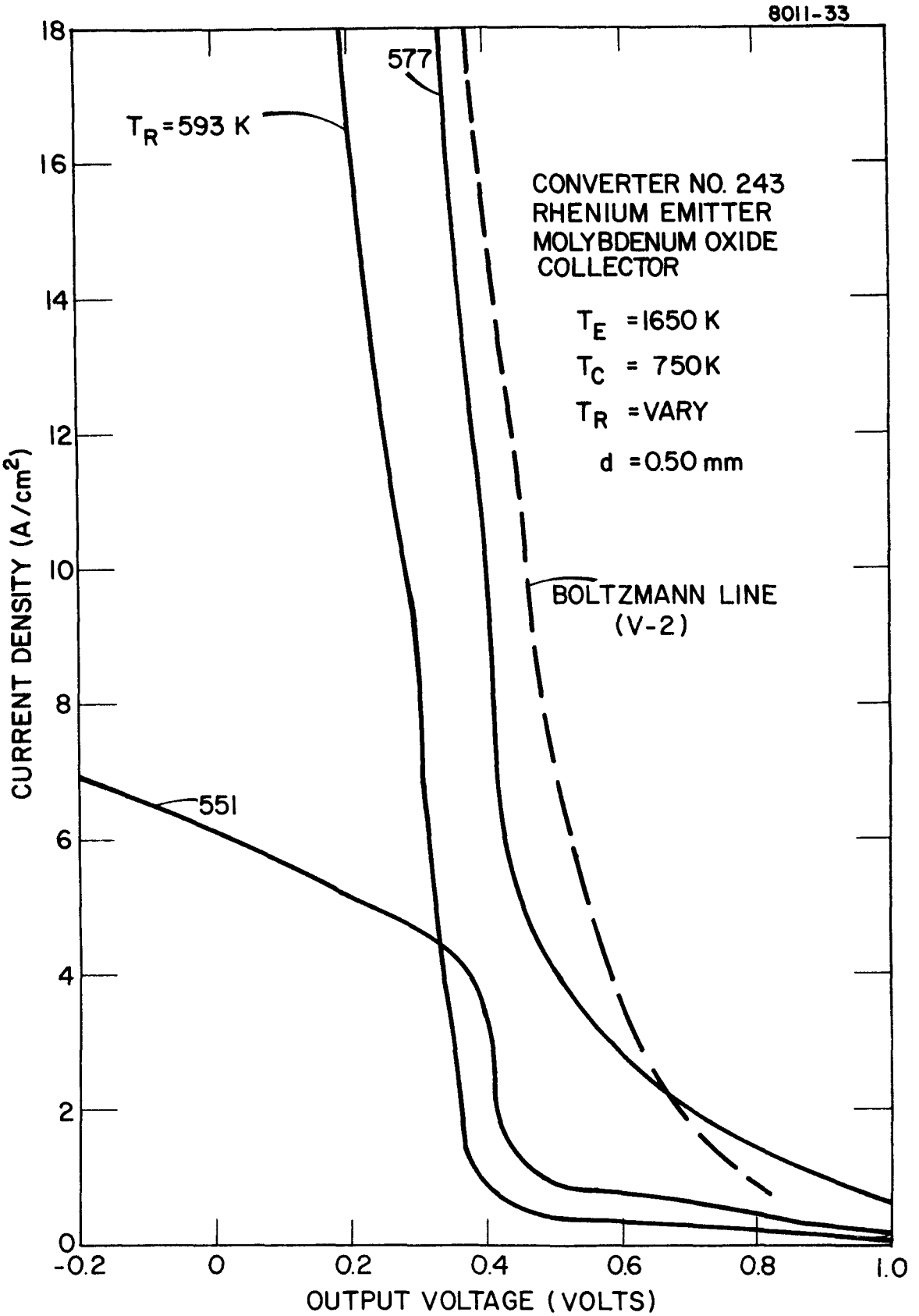


Figure 25. Cesium Reservoir Temperature Family at $T_E$ = 1650 K; $T_C$ = 750 K; d = 0.50 mm for Converter No. 243

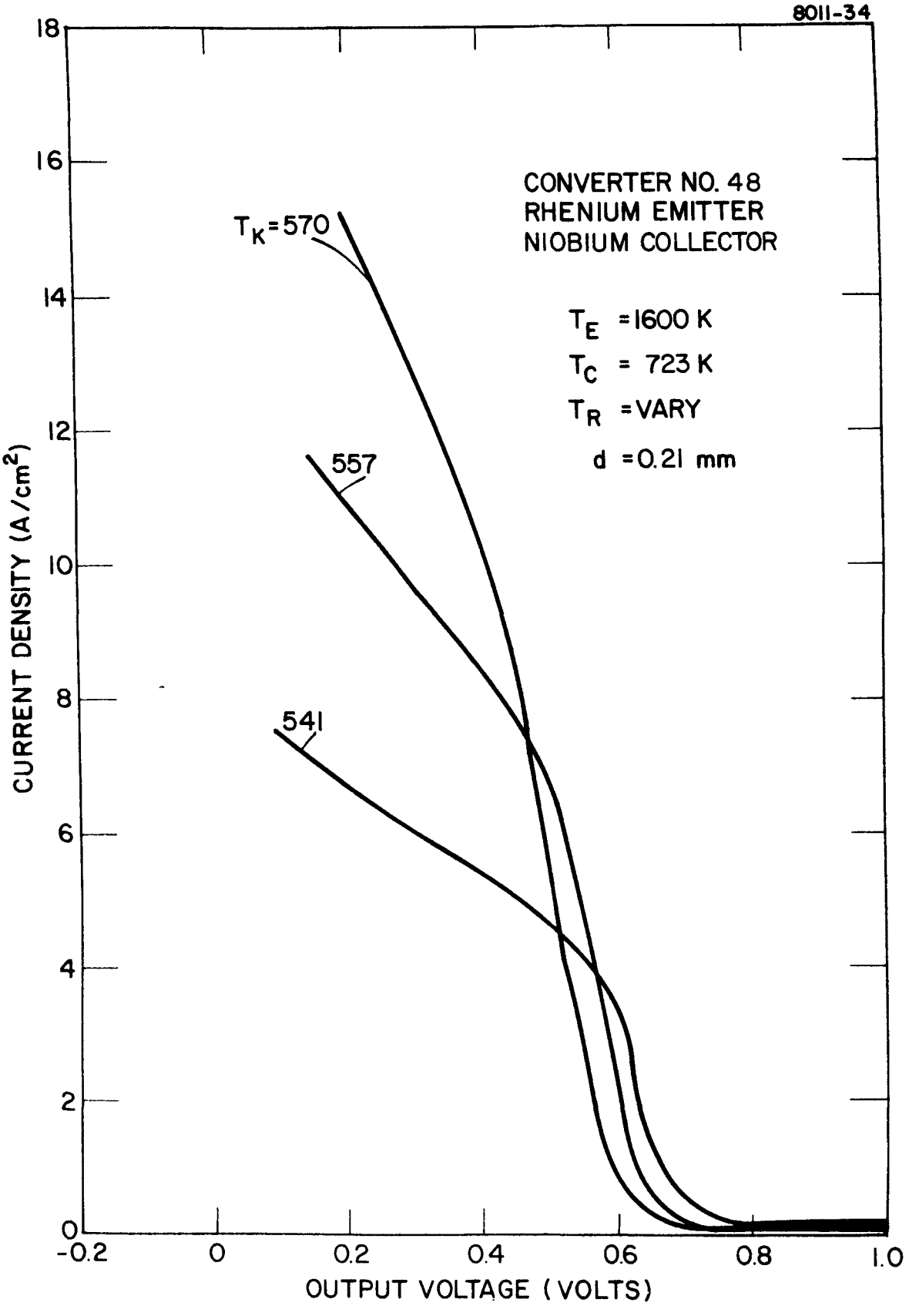


Figure 26. Cesium Reservoir Temperature Family at $T_E$ = 1600 K; $T_C$ = 723 K and d = 0.21 mm for Converter No. 48

### 2.1.2 TASK IX. ADVANCED CONVERTER STUDIES

In the conventional ignited mode diode, transport losses due to ionization, and coulombic and neutral atom scattering greatly reduce conversion efficiency. The objective of this task is to demonstrate improved thermionic converter performance by means of reduced potential loss in the interelectrode space. Based on previous studies, the particle thermionic converter (PTC) has been chosen for further investigations. Specifically, the electrical and thermal properties of PTC configurations will be tested as a function of particle composition and electrode spacing.

Due to program priorities set by JPL, no significant effort was expended on this task during this reporting period.

### 2.1.3 TASK X. POSTOPERATION DIAGNOSTICS

The variable spaced planar converters built for JPL are deliverable items. However, if it appears advisable on mutual agreement between JPL and Thermo Electron, selected converters shall be opened for postoperational diagnostics after performance testing. The objective will be to identify the degradation mode, if any, and identify the probable mechanisms of formation.

The thermionic performance data of Converter No. 241 are given in Section 2.1.1 of this report. This diode had an as deposited CVD fluoride tungsten emitter and a collector formed subliming molybdenum oxide onto a niobium substrate. The oxygen concentration (18,000 ppm by weight) was the highest that has been tested. After approximately 10 hours of operation, an electrical short caused by delamination of the deposited collector surface terminated converter testing.

The collector fabrication consisted of two steps. First, a thin layer of molybdenum (approximately of 0.5 mils) was evaporated onto the niobium substrate in a vacuum of $1 \times 10^{-6}$ torr. Next, oxygen was introduced to a pressure of $8 \times 10^{-5}$ torr and the molybdenum rod heated until a coating thickness of about 16 mils was deposited on the niobium.

Postoperatively, the collector deposit (see Figure 27) showed extensive cracking and spalling. A photomicrograph of a cross section through the collector is shown in Figure 28. It shows that the coating is porous and is poorly adherent. A chemical analysis of coating chips from Converter No. 241 is given in Table II. This analysis was performed by Luvak, Inc. of Boylston, Massachusetts. These data indicate that the oxygen concentration of the coating was not significantly depleted as the result of converter operation.

The distribution of cesium in the coating was measured by electron probe microanalysis. The line scan data are shown in Figure 29. Evidently, cesium rapidly penetrates the deposit either by diffusion or chemical reaction with the molybdenum oxide. The reduced cesium content near the surface is probably a consequence of heating the diode to drive cesium out of the electrode region prior to opening it for diagnostics.

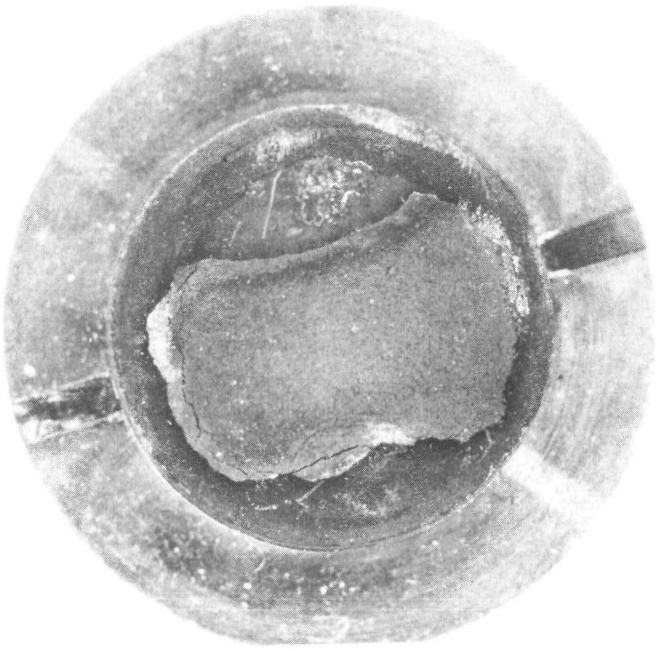

Figure 27. Photograph Shows Cracked and Spalling Collector Deposit

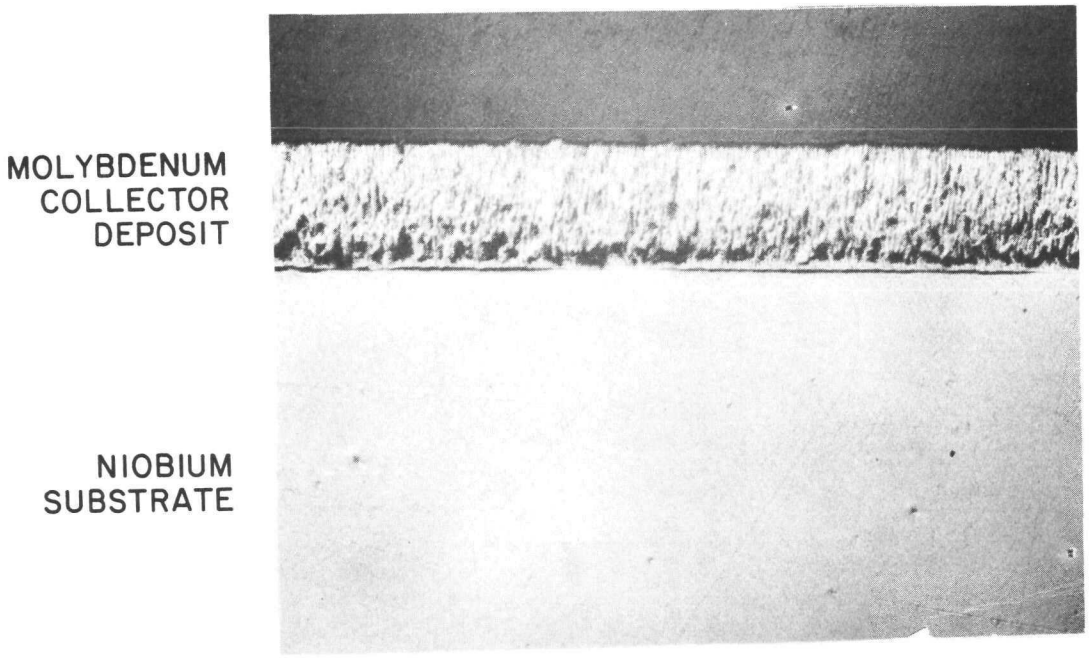


Figure 28. Photomicrograph Shows Poor Adhesion of Deposit to Niobium Substrate and Porosity in the Deposit

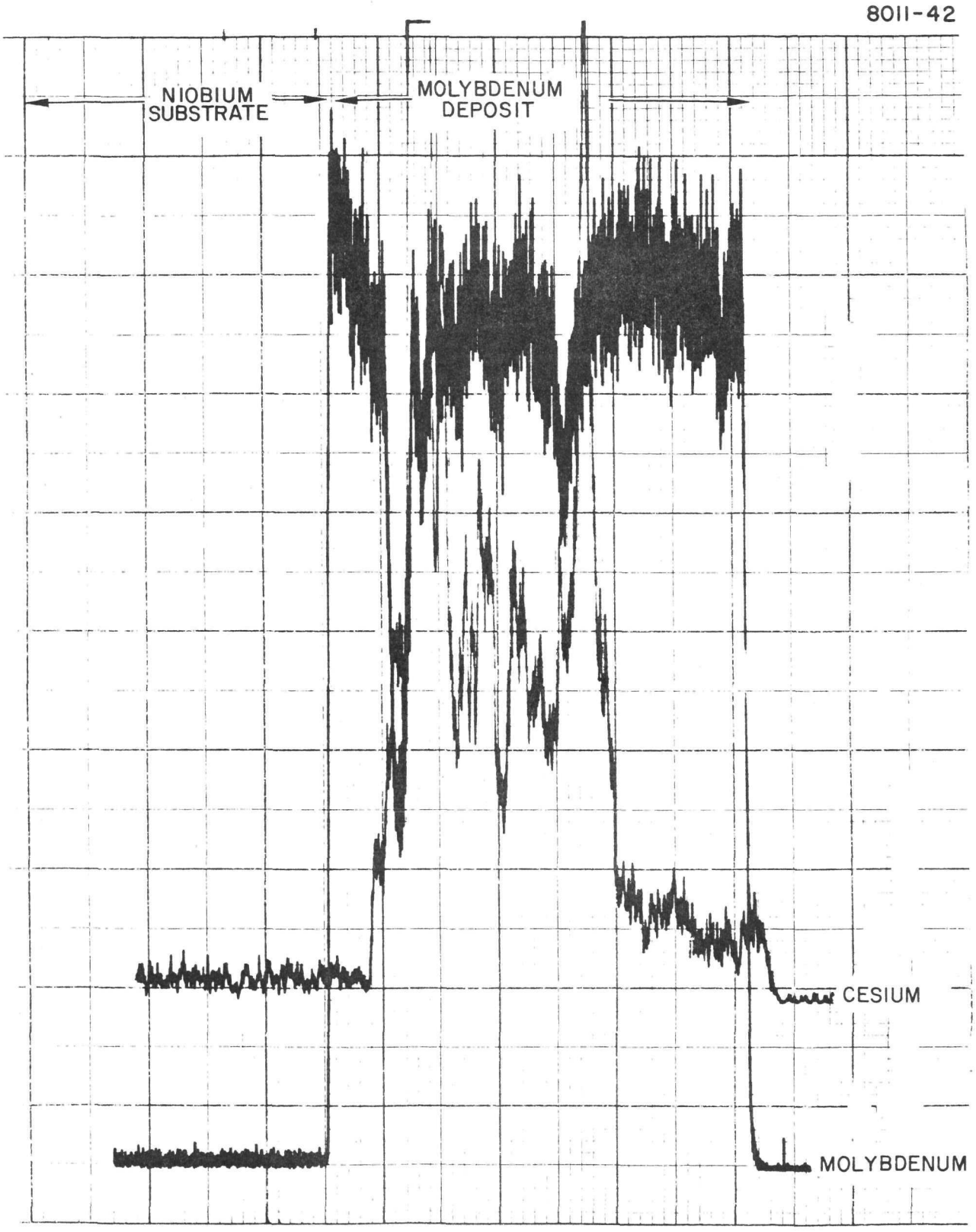


Figure 29. Cesium Line Scan in Collector Deposit

TABLE II

CHEMICAL ANALYSIS OF COLLECTOR COATING
OF CONVERTER NO. 241

| ELEMENT | PERCENT | PPM |
|---|---|---|
| Molybdenum | Major | Major |
| Oxygen | 2.08 | 20,800 |
| Cesium | .4 | 4,000 |
| Carbon | < .03 | < 300 |
| Silicon | .14 | 1,400 |
| Magnesium | .002 | 20 |
| Aluminum | .03 | 300 |

## 2.2 CYLINDRICAL CONVERTER DEVELOPMENT

### 2.2.1 TASK XI. CYLINDRICAL CONVERTER COMPONENT DEVELOPMENT

The objective of this task is to develop the technology required to construct cylindrical converters, excluding the electrode surfaces. This task includes electrode insulation, seal-bellows subassembly and thermoelectric lead components.

Due to program priorities established by JPL, no significant effort was expended on this task during this reporting period.

### 2.2.2 TASK XII. CORRELATION OF DESIGN INTERFACES

The objective of this task is to provide technical coordination between Thermo Electron and other contractors as well as with government agencies in order to assure overall compatibility of design, materials and interfaces between the thermionic conversion and other subsystems.

In view of the difficulty in obtaining a long-life electrical insulation of the heat pipe and thermionic converter emitter structure, an alternative coupling mechanism has been investigated. A preliminary computer analysis has been performed to model radiation coupling between the emitters and the reactor heat pipes.

Several system configurations were studied, as follows:

1. Insulated system with emitter and collector heat pipes

2. Radiation coupled system with emitter and collector heat pipes

3. Radiation coupled system with integral heat receiver and radiator with refractory wall

Configuration 1 has been studied before. The results have been presented in Reference 2. Configuration 2 is similar to Configuration 1, where the insulator is replaced with a radiation gap. This configuration is impractical since the heat flux transmitted at the heat pipe temperature is far below that required to operate

the thermionic converters at the design point. The schematic arrangement of Configuration 3 is shown in Figure 30. The reactor heat pipes form a bundle at the center of the spacecraft. The radiated heat is received by a heat receiver which is integral to the emitter structure. The area of the heat receiver is assumed to be four times the area of the emitter. The collector reject heat is radiated to space by an integral collector radiator as shown in Figure 31. The specific masses of the system have been calculated for barrier indices of 2.1, 2.0, and 1.95 eV to be 25.2, 24.0, and 21.9 kg/kWe; respectively. Further details of the analysis are shown in Table III. An analysis was also performed for a system with a refractory wall placed near the reactor heat pipe, as shown in Figure 30. The results were similar to the case without the refactory wall.

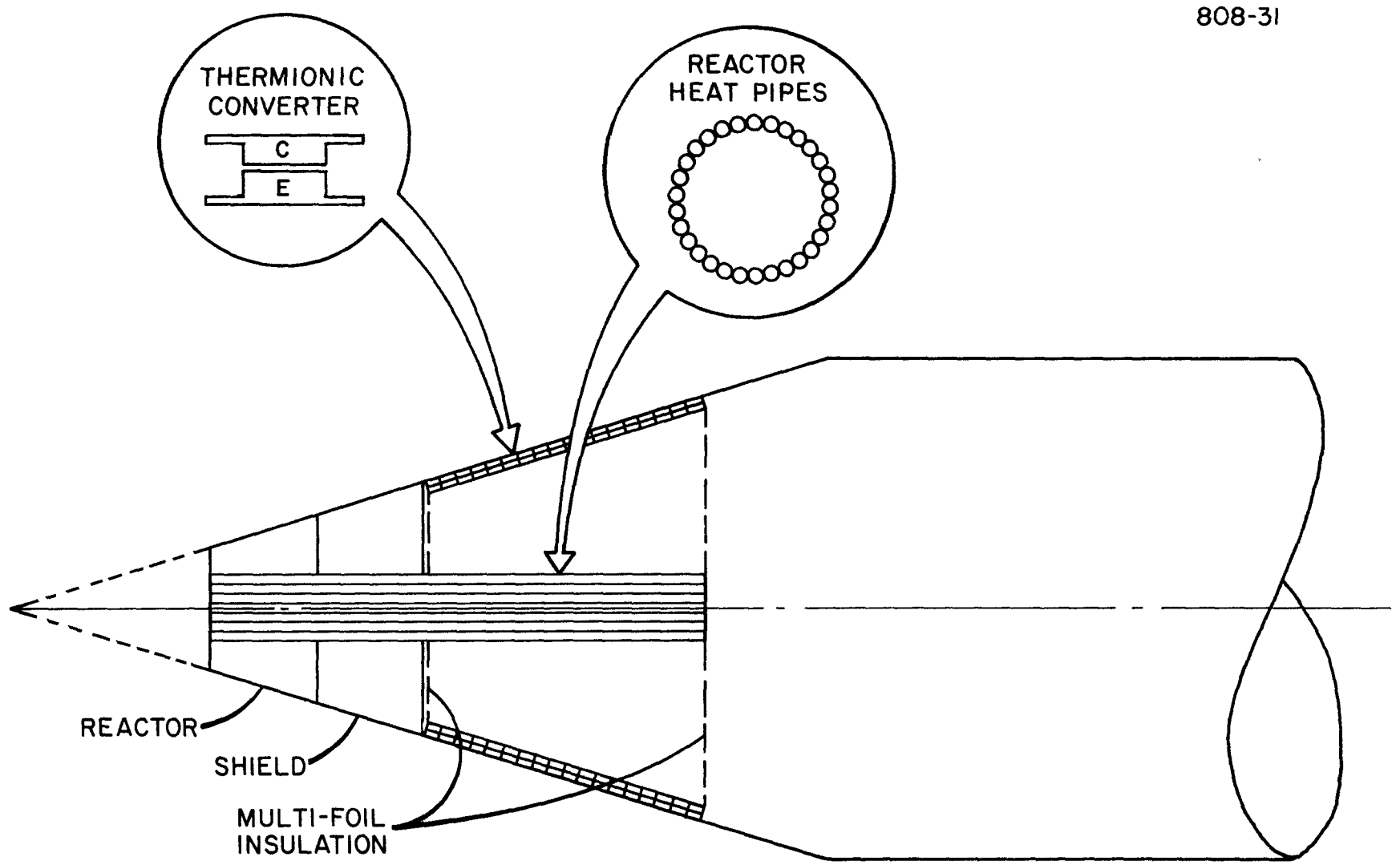


Figure 30. Spacecraft Configuration with Thermionics Integral Radiator and Heat Receiver

806-16

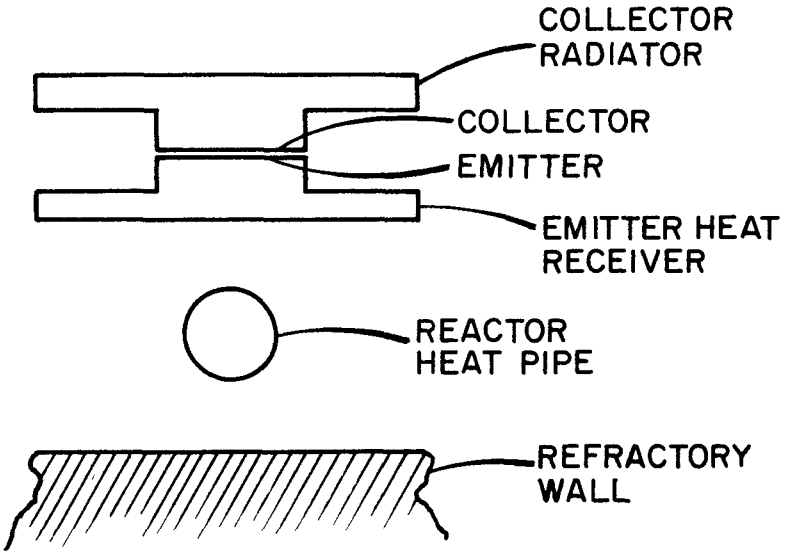


Figure 31. Model for Radiant Coupled Thermionic Space Power System

# TABLE III

## SYSTEM SPECIFIC MASS RESULTS

## RADIATION COUPLED SYSTEM WITH INTEGRAL RADIATOR AND HEAT RECEIVER

TOTAL POWER OUTPUT 120 kW
HEAT PIPE TEMPERATURE 1675 K

| $T_E$ = 1600 K<br>$T_C$ = 900 K<br>J = 2 A/cm | $V_B$ = 2.1 eV<br>$V_d$ = 0.5 eV<br>D = 2 cm<br>L = 30 cm<br>t = 0.15 cm | $V_B$ = 2.0 eV<br>$V_d$ = 0.5 eV<br>D = 2 cm<br>L = 28 cm<br>t = 0.15 cm | $V_B$ = 1.95 eV<br>$V_d$ = 0.4 eV<br>D = 2 cm<br>L = 22 cm<br>t = 0.15 cm |
|---|---|---|---|
| LEAD EFFICIENCY % | 8.9 | 9.9 | 11.9 |
| MASSES (kg) | | | |
| REACTOR | 524 | 501 | 467 |
| REACTOR HEAT PIPES | 795 | 768 | 705 |
| CONVERTERS | 992 | 889 | 741 |
| STRUCTURE | 95 | 95 | 95 |
| SHIELD | 541 | 541 | 541 |
| MISCELLANEOUS | 80 | 80 | 80 |
| TOTAL MASS (Kg) | 3027 | 2874 | 2629 |
| SPECIFIC MASS (Kg/kWe) | 25.2 | 24.0 | 21.9 |

## REFERENCES

1. L.R. Danielson and L.W. Swanson, "High Temperature Coadsorption Study of Zirconium and Oxygen on the W(100) Crystal Face," Surface Sci. 88 14-30 (1979).

2. DOE/JPL Advanced Thermionic Technology Program, Progress Report No. TE 4258/4247-226-80, March 1980.